Clim Dyn
DOI 10.1007/s00382-007-0258-5

Causes and impacts of changes in the Arctic freshwater budget during the twentieth and twenty-first centuries in an AOGCM

Olivier Arzel · Thierry Fichefet · Hugues Goosse · Jean-Louis Dufresne

Received: 5 September 2006 / Accepted: 30 March 2007

Abstract The fourth version of the atmosphere-ocean general circulation (AOGCM) model developed at the Institut Pierre-Simon Laplace (IPSL-CM4) is used to investigate the mechanisms influencing the Arctic freshwater balance in response to anthropogenic greenhouse gas forcing. The freshwater influence on the interannual variability of deep winter oceanic convection in the Nordic Seas is also studied on the basis of correlation and regression analyses of detrended variables. The model shows that the Fram Strait outflow, which is an important source of freshwater for the northern North Atlantic, experiences a rapid and strong transition from a weak state toward a relatively strong state during 1990–2010. The authors propose that this climate shift is triggered by the retreat of sea ice in the Barents Sea during the late twentieth century. This sea ice reduction initiates a positive feedback in the atmosphere-sea ice-ocean system that alters both the atmospheric and oceanic circulations in the Greenland-Iceland-Norwegian (GIN)-Barents Seas sector. Around year 2080, the model predicts a second transition threshold beyond which the Fram Strait outflow is restored toward its original weak value. The long-term freshening of the GIN Seas is invoked to explain this rapid transition. It is further found that the mechanism of interannual changes in deep mixing differ fundamentally between the twentieth and twenty-first centuries. This difference is caused by the dominant influence of freshwater over the twenty-first century. In the GIN Seas, the interannual changes in the liquid freshwater export out of the Arctic Ocean through Fram Strait combined with the interannual changes in the liquid freshwater import from the North Atlantic are shown to have a major influence in driving the interannual variability of the deep convection during the twenty-first century. South of Iceland, the other region of deep water renewal in the model, changes in freshwater import from the North Atlantic constitute the dominant forcing of deep convection on interannual time scales over the twenty-first century.

O. Arzel (✉)
Climate and Environmental Dynamics Laboratory,
School of Mathematics and Statistics,
University of New South Wales,
Sydney, NSW 2052, Australia
e-mail: o.arzel@unsw.edu.au

T. Fichefet · H. Goosse
Institut d'Astronomie et de Géophysique G. Lemaître,
Université catholique de Louvain, 2 Chemin du Cyclotron,
1348 Louvain-la-Neuve, Belgium

J.-L. Dufresne
Laboratoire de Météorologie Dynamique,
Institut Pierre Simon Laplace UPMC/CNRS,
4, place Jussieu, Paris, France

1 Introduction

The freshwater supply to the Arctic Ocean plays a key role in controlling the circulation and water mass properties of this ocean. Furthermore, the export of this freshwater toward the convection sites located in the Labrador and Greenland–Iceland–Norwegian (GIN) Seas significantly affects deep water formation (e.g., Manabe and Stouffer 1995; Hakkinen 1999; Jungclaus et al. 2005) and ultimately the Atlantic meridional overturning circulation (AMOC). Excessive freshwater input to the Arctic Ocean and Nordic Seas could thus influence the climate of the North Atlantic area by decreasing the northward ocean heat transport associated with the large-scale AMOC (e.g., Vellinga and

Wood 2002; Fichefet et al. 2003). The present study aims at increasing our understanding of the mechanisms of freshwater release from the Arctic Ocean towards sub-Arctic regions on decadal and longer timescales in response to enhanced greenhouse gas conditions. In addition, the interrelation between changes in freshwater transport toward the convection sites and winter deep oceanic convection on interannual time scales is addressed.

During the last few decades, the physical Arctic environment has undergone large changes, as reviewed in recent literature (e.g., Serreze et al. 2000; Moritz et al. 2002; Overland et al. 2004). For example, since the mid-1960s, the annual mean Arctic surface air temperature has increased by approximately 2°C. Since the late 1970s, satellite records show a decreasing linear trend in Arctic sea ice extent at an annual mean rate of about 0.3×10^6 km^2 per decade (Cavalieri et al. 2003). Submarine-based observations indicate that the sea ice thickness in deep water areas of the Arctic Ocean has decreased by roughly 1.3 m in average between 1958–1976 and 1993–1997 (Rothrock et al. 1999). River monitoring data show that the average annual discharge of freshwater from the six largest Eurasian rivers to the Arctic Ocean has increased by about 7% from 1936 to 1999, suggesting an increase of precipitation over land in high latitudes of the Northern Hemisphere during that period (Peterson et al. 2002). Hansen et al. (2001) reported that one of the cold, dense overflows across the Greenland–Scotland ridge that feeds the southward branch of the AMOC, has decreased by at least 20% during 1950–2000. Dickson et al. (2002) presented evidence of a rapid and sustained freshening of the system of overflows and entrainment that ventilate the deep Atlantic Ocean over 1965–2000. Curry et al. (2003) found systematic freshening over much of the water column at both poleward ends of the Atlantic Ocean, accompanied by large increases of salinity in the upper water column at low latitudes between the 1950s and the 1990s. Recently, Curry and Mauritzen (2005) estimated that the Nordic Seas and the sub-polar basins were diluted by an extra 19,000 ± 5,000 km^3 of freshwater input between 1965 and 1995, with about half of this freshwater being added in the late 1960s at a rate of 2,000 km^3 per year during the Great Salinity Anomaly (GSA) event (Dickson et al. 1988).

Whether the high-latitude freshening and the reduced overflows observed during the past four decades are a manifestation of a weakening of the AMOC remains very controversial. Indeed, the relationship between the large-scale AMOC and the northern North Atlantic freshening is difficult to infer from current observations because of the overall lack of data and the too short period of measurements compared to timescales of internal variability. Nevertheless, using five transatlantic sections at 25°N, Bryden et al. (2005) suggested recently that the AMOC has slowed down by about 30 percent between 1957 and 2004. This contrasts with the studies of Knight et al. (2005) and Latif et al. (2006) that do not support evidence of a persistent weakening of the AMOC during the last few decades, therefore sustaining some controversy on the current state of the AMOC (Kerr 2005). Using the HadCM3 climate model running over the twentieth century, Wu et al. (2004) reported a deep freshening trend of the Labrador Sea similar to that seen in observations by Dickson et al. (2002), and yet obtained an enhancement of the AMOC instead of a weakening. The situation is however very different over the twenty-first century for which the radiative forcing is much larger than the one experienced over the second half of the past century. In this case models show unequivocally, albeit with various magnitudes, a weakening of the AMOC in response to increasing anthropogenic greenhouse gas forcing (e.g., Houghton et al. 2001; Fichefet et al. 2003; Gregory et al. 2005). It is worth noting that in all models used in the Coupled Model Intercomparison Project (CMIP), the AMOC weakening is caused more by changes in surface heat flux than by changes in surface freshwater flux (Gregory et al. 2005). However, increase in both sea ice melting and river flows are generally found in these climate-change scenarios, leading to an increase in the freshwater storage of the Arctic/sub-Arctic regions. As a result, the high-latitude ocean stratification increases and the water mass transformation becomes much less efficient, thereby contributing to the AMOC weakening.

Although models agree that the northern North Atlantic freshens in response to global warming, the mechanisms driving the changes in freshwater release on decadal or longer timescales from the Arctic Ocean to the Nordic Seas and the sub-polar basin of the North Atlantic are not well understood. On interannual timescales, the influence of freshwater on deep convection in a warming climate has not yet been established. The present analysis is a first step towards understanding these mechanisms. The first objective is to gain an insight into the processes governing the oceanic freshwater export from the Arctic basin to the high latitudes of the northern North Atlantic in response to enhanced greenhouse gas conditions. We especially focus our analysis on the freshwater export at Fram Strait which represents the main source of freshwater for the sub-polar basin of the North Atlantic Ocean. The second objective is to determine whether the mechanisms responsible for the interannual variability of deep winter oceanic convection over the twentieth century are also valid over the twenty-first century. A deliberate emphasis is put on the influence of interannual changes in oceanic freshwater fluxes at boundaries enclosing the convection sites. It should be

stressed that this second analysis is based on detrended variables so that the results do not depend on the long-term trends induced by the climate change experienced over the twenty-first century, such as the long-term freshening of the high latitudes for instance. However, the non linear impact of the freshening on the oceanic properties such as stratification or vertical mixing for instance is not removed by this linear detrending. The analysis is based on outputs of simulations performed with an atmosphere-ocean general circulation model for the fourth assessment report of the Intergovernmental Panel on Climate Change (IPCC AR4). In this paper, we discuss results from the experiment covering the twentieth century with anthropogenic forcings and the A1B scenario for the twenty-first century, which corresponds to an increase of CO2 until a level of 720 ppm by 2100 as defined by the Special Report on Emission Scenario (SRES).

After a brief description of the coupled climate model and its climatology in Sects. 2 and 3, respectively, the freshwater budget of the Arctic Ocean over the twentieth and twenty-first centuries is presented in Sect. 4. Section 5 deals with the mechanisms influencing the long-term changes in the liquid freshwater transport out of the Arctic Ocean through Fram Strait, while Sect. 6 is devoted to the mechanisms governing the interannual variability of deep oceanic convection over the twentieth and twenty-first centuries. Conclusions are finally given in Sect. 7.

2 Model description and experimental design

We use the fourth version of the AOGCM developed at the ''Institut Pierre Simon Laplace'', Paris (IPSL-CM4, Marti et al. 2005). This model is made up of the atmospheric general circulation model LMDz (Hourdin et al. 2006), the oceanic general circulation model ORCA (Madec et al. 1998), the thermodynamic–dynamic sea ice model LIM (Fichefet and Morales Maqueda 1997) and the land surface scheme ORCHIDEE (Krinner et al. 2005). Time synchronisation and spatial interpolation of surface fluxes and variables between the atmospheric model and the three other components are ensured through the OASIS coupler (Valcke et al. 2004). There is no flux correction in this model. The fresh water associated with ice sheet melting is drained toward the ocean and does not affect the ice sheet geometry (no dynamics). The atmospheric model has a horizontal resolution of 3.75° in longitude and 2.5° in latitude, with 19 levels along the vertical. The oceanic model has a coarse horizontal resolution of 2° in longitude and latitude, with vertical grid spacing increasing from 10 m in the top 150 m to 500 m at the bottom (31 levels).

The outputs from the experiment covering the twentieth century, which includes only the anthropogenic forcing (observed greenhouse gases and sulphate aerosol concentrations), are first discussed. For the twenty-first century, we use outputs from the SRES A1B climate change scenario which corresponds to a continuous increase of CO_2 concentration until a level of about 720 ppm by 2100. A detailed description of those simulations is provided in Dufresne et al. (2005).

3 Climatology of the Arctic Ocean

A description of the model climatology can be found in Swingedouw et al. (2006). A summary is given here for the reader's convenience, with a particular focus on the Arctic Ocean over the period 1951–2000. The geometry of the Arctic Ocean is defined in Fig. 1. As in most AOGCMs, IPSL CM4 has several biases in its mean climate compared to observations. The AMOC index, defined as the maximum value of the annual mean meridional overturning streamfunction between 500 and 5,000 m depth in the Atlantic basin, has a small linear trend of –0.17 Sv per decade over 1951–2000 and a mean annual value of 11.8 ± 0.7 Sv. These statistics are close to those simulated in the pre-industrial control run over the same reference period (12 ± 0.9 Sv with a trend of –0.14 Sv per decade). This is somewhat weaker than the observational estimates

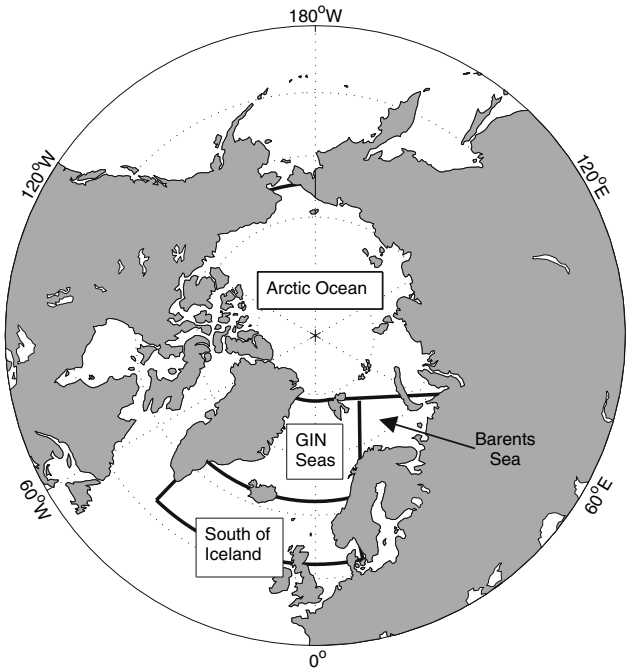

Fig. 1 Location map showing the geometry of the three boxes chosen for the present study. These include the Arctic Ocean, the Greenland–Iceland–Norwegian Seas and the region located south of Iceland. These latter two enclose the regions where the winter deep oceanic convection occurs over the twentieth century in the model (see Fig. 2)

of 15 ± 2 Sv reported by Ganachaud and Wunsch (2000). Swingedouw et al. (2006) mostly attributed this error to an excess of precipitation minus evaporation between 45° and 50°N that leads to too low sea surface salinities (SSS) in the northern North Atlantic. The largest SSS bias occurs at mid-latitudes and underestimate the Levitus (1994) climatology by about 2 psu. In the Labrador Sea, this results in the formation of a strong halocline that prevents deep winter oceanic convection. Deep water renewal in the model occurs in the GIN Seas in agreement with observations (Dickson et al. 1996) and south of Iceland, east of the Irminger Sea (Fig. 2). This second location of deep water formation differs from the one deduced by Pickart et al. (2003) from observations, that is in the southwestern Irminger Sea. The good agreement between the simulated outflow rate of water denser than 27.8 kg m^{-3} over the Greenland–Iceland–Scotland ridge (5.4 Sv) and observations (5.6 Sv, Dickson and Brown 1994) suggests that the AMOC bias is instead related to the absence of convection in the Labrador Sea (Swingedouw et al. 2006). This latter feature is accompanied by too large a sea ice extent in the Labrador Sea during winter (Fig. 3a). In summer, however, the sea ice edge location agrees reasonably well with observations (Fig. 3b). It should be noted that the too weak AMOC simulated by the model is also associated with a cold bias of about 5°C in the northern North Atlantic (45–50°N).

The mean sea ice velocities computed by the model (not shown) are in reasonable agreement with those derived from the 85.5 GHz Special Sensor Microwave/Imager (SSM/I) data by Emery et al. (1997). The sea ice drift features the Beaufort Gyre, the Transpolar Drift, the divergent motion on the Siberian shelf and the sea ice export through Fram Strait. The simulated large-scale ocean surface circulation (not shown) displays roughly the same features as the mean sea ice drift pattern in the Arctic Ocean, namely the Beaufort Gyre, the Transpolar Drift stream and the East Greenland Current. Both the Bering Strait inflow in the Arctic Ocean (1 Sv) and the Canadian Arctic Archipelago throughflow (0.7 Sv) are

Fig. 2 Simulated mixed layer depth in March averaged over 1951–2000. Contours are shown for values of 100, 200, 300, 400, 500 and 1,000 m

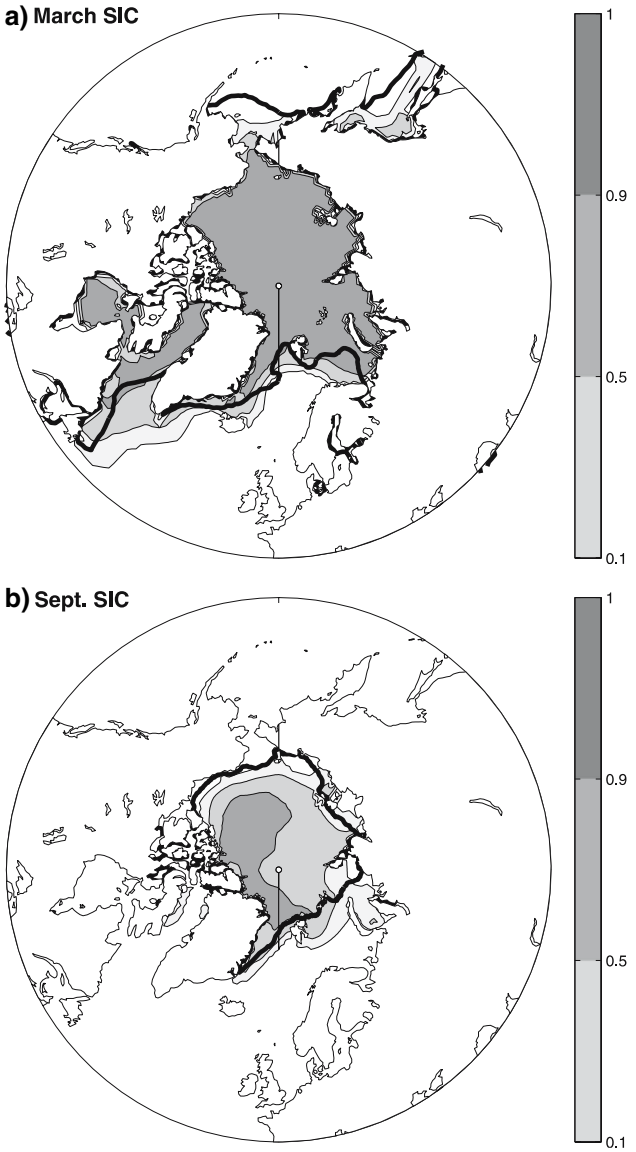

Fig. 3 Sea ice concentrations (fraction) in March (top) and September (bottom) simulated by IPSL-CM4 averaged over 1951–2000. Only the contours 0.1, 0.3 and 0.9 are shown. The observed sea ice edge, derived from the HadISST dataset (Rayner et al. 2003), is defined as the 15 concentration for March and September and shown as a *thick solid line*

close to observational data. In the GIN Seas, a cyclonic gyre is simulated, but the inflow of Atlantic waters into the Barents Sea appears too small (0.17 Sv) compared to observational estimates of Blindheim (1989), which rather give a value of about 3 Sv. This model deficiency is mostly related to the too weak AMOC simulated by the model. The Fram Strait outflow (0.5 Sv) is therefore weaker than the one observed (3 Sv) in order to balance the mass budget of the Arctic Ocean. Consequently, the modeled Arctic Ocean is somewhat isolated from the northern North Atlantic.

4 Simulated Arctic freshwater budget over the twentieth and twenty-first centuries

In this section, we describe the modeled volume-averaged freshwater balance of the Arctic Ocean over 1951–2000 and 2051–2100 (Fig. 4). These 50-year periods have been chosen to avoid potential biases related to the large Arctic climate decadal variability in the model. For instance, the sea ice volume in the northern hemisphere shows significant variability at a period of 24 years over the twentieth century and 10 years over the twenty-first century. A reference salinity of 34.8 psu has been adopted to compute the freshwater fluxes. This peculiar value is a reasonable estimate of the average salinity of the Arctic Ocean and is usually the one used in oceanic freshwater related studies. Using such a value allows therefore a direct comparison of the freshwater budget simulated by our model with other model studies and observations (Serreze et al. 2006). If the salinity of the freshwater flux (at the boundary of the Arctic Ocean) is greater (smaller) than the reference salinity, the flux represents a freshwater sink (source) to the Arctic Ocean. It should be noted that this reference salinity is somewhat greater than the average Arctic salinity in the model, which is 34.64 psu over 1951–2000. Using the 34.64 reference instead of the usual 35.8 one slightly affects the overall picture of the freshwater budget presented in Fig. 4.

4.1 Definitions of freshwater storages and fluxes

The liquid freshwater stored (LFWC) in a given volume is defined as

$$\mathrm{LFWC} = \int \mathrm{d}V(S_{\mathrm{ref}} - S)/S_{\mathrm{ref}},$$

where S is the salinity and $\mathrm{d}V$ the volume increment. Note that the freshwater storage ignores the waters saltier than the 34.8 reference for which the equivalent freshwater storage is negative. The sea ice model in IPSL-CM4 assumes a constant sea ice salinity S_{ice} of 4 psu, the volume of freshwater stored in sea ice (i.e., solid freshwater content, SFWC) is then simply determined by

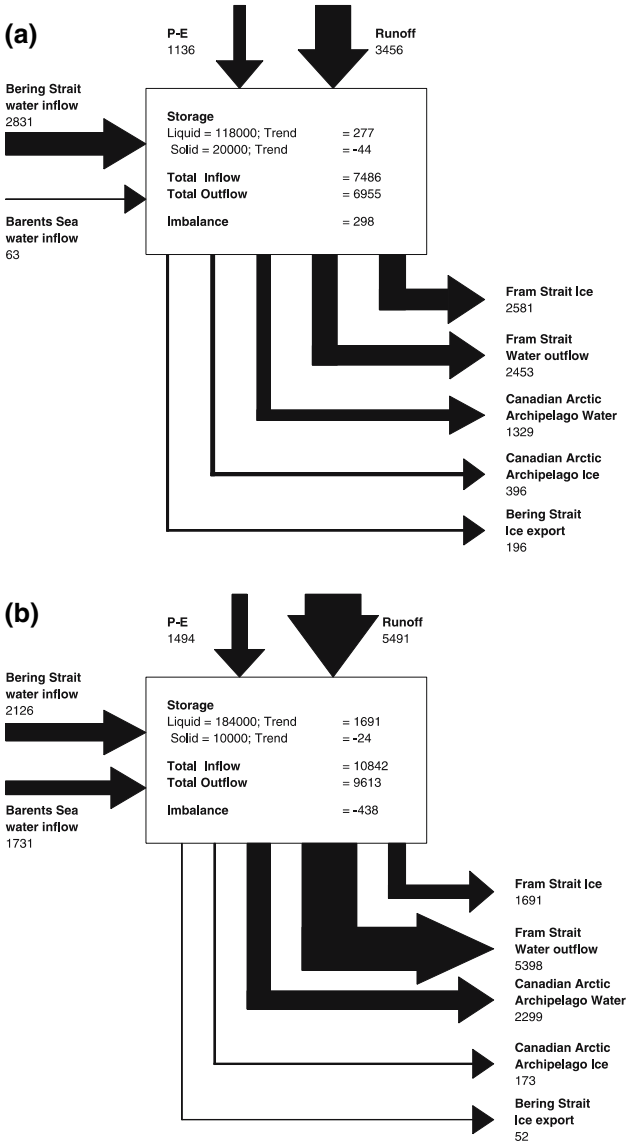

Fig. 4 Simulated annual mean freshwater budget in the Arctic Ocean (Fig. 1) averaged over the periods 1951–2000 (**a**) and 2051–2100 (**b**). Units are $\mathrm{km}^3\,\mathrm{year}^{-1}$ for all fluxes and trends, while stores are expressed in km^3. Note that the trend of freshwater storage here is the sum of the trends of ''positive'' and ''negative'' freshwater content (salinity smaller and greater than 34.8 psu, respectively) since we must take into account all the salinities for the freshwater budget estimate. The trend of the ''positive'' freshwater content represents a significant fraction of the total trend, 92 and 96% over the twentieth and twenty-first centuries, respectively. The width of the arrows is proportional to the value of the fluxes. The residual freshwater transport (imbalance), owing to the sub-monthly variability of sea ice, salinity and ocean currents, is also provided. A positive (negative) imbalance mean that more (less) freshwater leaves the central Arctic Ocean than enters it. See text for further details. Note that the sea ice-ocean freshwater flux vanishes when considering the total (i.e., liquid + solid) freshwater balance

$$\mathrm{SFWC} = V_{\mathrm{ice}}(S_{\mathrm{ref}} - S_{\mathrm{ice}})/S_{\mathrm{ref}},$$

where V_{ice} is the sea ice volume. The vertically integrated liquid freshwater transport (LFWT) through a vertical section of area increment dA is defined as

$$\mathrm{LFWT} = \int \mathrm{d}A\boldsymbol{u} \cdot \boldsymbol{n}(S_{\mathrm{ref}} - S)/S_{\mathrm{ref}},$$

where $\boldsymbol{u}$ is the horizontal velocity field and $\boldsymbol{n}$ the unity vector normal to the vertical section. Finally, the sea ice (solid) freshwater transport (SFWT) through a horizontal section reads

$$\mathrm{SFWT} = \int \mathrm{d}lhC_{\mathrm{ice}}\boldsymbol{u}_{\mathrm{ice}} \cdot \boldsymbol{n}(S_{\mathrm{ref}} - S)/S_{\mathrm{ref}},$$

where h, $\boldsymbol{u}_{\mathrm{ice}}$ and C_{ice} are the sea ice thickness, velocity and concentratrion distributions along the horizontal section of length increment dl, respectively, and n the unity vector normal to this section.

It should be noted that the calculation of freshwater fluxes is based on monthly outputs which do not allow by themselves to close the total (solid plus liquid) freshwater budget since the eddy fluxes owing to the sub-monthly variability of ocean currents, salinity and sea ice are missing. The computation of these terms would require online calculations during the course of the integration and were not made available for the present study that is based on experiments especially designed for the IPCC AR4 which already produce a large amount of data. This therefore introduces an uncertainty in the modeled oceanic freshwater transport estimates. However, as seen in Fig. 4, the imbalance associated with the absence of these terms (298 km^3 year^{-1} over 1951–2000 and –438 km^3 year^{-1} over 2051–2100) is an order of magnitude smaller than the major sources or sinks of fresh water. The method employed here to estimate the freshwater budget in the Arctic Ocean appears therefore as a suitable approximation.

4.2 Arctic Ocean freshwater budget over 1951–2000

Figure 4a illustrates the simulated annual mean freshwater budget of the Arctic Ocean over 1951–2000, while observations are provided in Table 1. Over this period, the mean liquid freshwater storage in the Arctic Ocean simulated by the model (118,000 km^3) overestimates the observational estimates of Aagaard and Carmack (1989) and Serreze et al. (2006) by 38,000 km^3 and 41,000 km^3, respectively. The bias is mainly apparent in the eastern part of the Arctic basin and is likely caused by the relatively weak AMOC simulated by the model that does not support an inflow of salty waters (i.e., saltier than the 34.8 reference) through the Barents Sea. The volume of freshwater stored in sea ice (20,000 km^3) compares however reasonably well with the value of 17,300 km^3 estimated by Aagaard and Carmack (1989). Note that the trend of liquid freshwater content simulated over 1951–2000 (277 km^3 year^{-1}) contrasts with that obtained over 1901–1950 (–34 km^3 year^{-1}). No significant trends could be found in the pre-industrial control run indicating that the long-term freshening of the Arctic Ocean initiated over the second half of the twentieth century in the model results from anthropogenic effects. The trends of solid freshwater fluxes over 1901–1950 and 1951–2100 are –22 km^3 year^{-1} and –44 km^3 year^{-1}, respectively, but are not significant given the large variability of Arctic sea ice volume over the twentieth century (annual standard deviation of about 2,100 km^3).

As a percentage of the total freshwater input to the Arctic Ocean (7,486 km^3 year^{-1}), the dominant terms are the river runoff (46%), the Bering Strait water inflow (38%), and the

Table 1 Observation-based estimates of annual mean oceanic freshwater fluxes for the Arctic Ocean relative to a salinity of 34.8 psu, river input and precipitation less evaporation

Term	Value	Period	Source
River input	3200 ± 110	1980–1999	Serreze et al. (2000)
P-E	2000 ± 200	1979–2001	ERA40 reanalysis
Bering Strait inflow	2500 ± 300	1990–2004	Woodgate and Aagaard (2005)
Canadian Arctic Achipelago water outflow	–3200 ± 320	1998–2000 + model	Prinsenberg and Hamilton (2005)
Canadian Arctic Achipelago ice outflow	–160	1998–2000	Prinsenberg and Hamilton (2005)
Fram Strait upper water outflow	–2400 ± 400	1997–1998	Meredith et al. (2001)
Fram Strait deep outflow	500 ± 130	Not available	Dickson et al. (2006)
Fram Strait ice outflow	–2300 ± 340	1990–1996	Vinje et al. (1998)
West Spitzbergen Current (Atlantic inflow)	–760 ± 320	1997–2000	Dickson et al. (2006)
Barents Sea Branch (Atlantic inflow)	–340 ± 80	1998–2001	Dickson et al. (2006)

Values are given in km^3 year^{-1}. Negative values mean freshwater outflows. Estimated errors, related to the lack of data, intrinsic variability and trends are also provided where available. All the values provided here are assumed to be the best estimates, as judged by Serreze et al. (2006)

net precipitation (15%). A weak liquid freshwater inflow through the Barents Sea (63 km^3 $year^{-1}$, 1% of the total) is simulated while observations reported by Dickson et al. (2006) rather show an annual mean export of 340 km^3 $year^{-1}$ there (Table 1). The magnitude of the river input (3,456 km^3 $year^{-1}$) is close to the value of 3,200 km^3 $year^{-1}$ estimated by Serreze et al. (2006). Through Bering Strait, a sea ice export of 196 km^3 $year^{-1}$ is simulated in contrast to the observations that show an inflow of 400 km^3 $year^{-1}$ (Woodgate and Aagaard 2005). However, the total (i.e., solid plus liquid) freshwater inflow at Bering Strait (2,635 km^3 $year^{-1}$) remains close to observation-based estimates (2,500 km^3 $year^{-1}$, Woodgate and Aagaard 2005). The underestimation of the net precipitation (1,136 km^3 $year^{-1}$), averaged over the Arctic Ocean, compared to the ERA40 reanalysis (2,000 km^3 $year^{-1}$) is the main cause of the lower than observed total inflow (8,500 km^3 $year^{-1}$, Serreze et al. 2006) of freshwater into the Arctic Ocean in the model.

The total freshwater outflow (6,955 km^3 $year^{-1}$) is largely dominated by the transport at Fram Strait (72%), followed by the transport through the Canadian Arctic Archipelago (25%) and the Bering Strait sea ice export (3%). At Fram Strait, the outflow is roughly equally partitioned between the solid and liquid contributions in agreement with observational data (Table 1). The annual mean ice export at Fram Strait (93,400 m^3 s^{-1}) compares quite well with data collected by Vinje et al. (1998) and Kwok et al. (2004). Finally, the strong agreement of the simulated liquid freshwater export at Fram Strait (2,453 km^3 $year^{-1}$) with observational-based estimates (Table 1) results from the compensation of two biases: the greater than observed liquid freshwater storage in the Arctic basin combined with the too weak Fram Strait volume flux (0.51 ± 0.44 Sv).

4.3 Arctic Ocean freshwater budget over 2051–2100

Figure 4b illustrates the mean annual freshwater budget of the Arctic Ocean in the model over 2051–2100. Compared to 1951–2000, the mean liquid freshwater storage over 2051–2100 (184,000 km^3) is increased by 56%, while its mean annual trend (1,691 km^3 $year^{-1}$) is mutiplied by 6. During the same period, the volume of freshwater stored in sea ice is 50% less, with a mean value of 10,000 km^3. It should be noted that the trend in sea ice volume, which is the same as the one in solid freshwater storage (since the sea ice salinity is constant), over 2051–2100 is weak (–24 km^3 $year^{-1}$) compared to 2001–2050 (–158 km^3 $year^{-1}$). This interesting behavior might be related to the negative feedback documented by Bitz and Roe (2004). This thermodynamic feedback implies that thinner ice does not need to thin as much than thicker ice to increase its growth rate. As a consequence, assuming that the sea ice volume changes are dominated by sea ice thickness changes rather than sea ice cover changes, the trend in sea ice volume would decrease along with the sea ice pack thickness when this latter is sufficiently small (i.e., from year 2050 onwards in our model). The total inflow (10,842 km^3 $year^{-1}$) and outflow (9,613 km^3 $year^{-1}$) of freshwater are 45 and 38% more than those simulated over 1951–2000, respectively. With the trends in freshwater storage, our results indicate therefore an imbalance of –438 km^3 $year^{-1}$, a small value compared to the dominant sources and sinks of freshwater (see Sect. 4.1 for further discussion).

The freshening of the Arctic Ocean is caused, with similar contributions, by the increases in continental runoff and the freshwater import from the Barents Sea. This enhanced river discharge into the Arctic Ocean (2,035 km^3 $year^{-1}$ = 0.065 Sv, or 59% relative change) is an indication of the increase in the integrated high-latitude net precipitation over continental areas resulting from an intensified hydrological cycle in response to global warming (Wu et al. 2005). The large shift seen in the freshwater import through the northern boundary of the Barents Sea into the Arctic basin (2,020 km^3 $year^{-1}$) results from the combined effect of the freshening in the GIN Seas and the strengthening of the northward volume flux through the Barents Sea. The change in the atmospheric freshwater flux (P-E) represents only a small contribution (358 km^3 $year^{-1}$) to the freshening of the Arctic Ocean. Liquid freshwater export at Fram Strait over the period 2051–2100 is more than twice that simulated over 1951–2000 and appears to dominate the sink of freshwater (–5,398 km^3 $year^{-1}$). Solid freshwater export at Fram Strait (1,691 km^3 $year^{-1}$) is however 35% less than over 1951–2000 in agreement with the net decrease in sea ice volume. The freshwater export through the Canadian Archipelago is enhanced by about 73% compared to 1951–2000, while the volume flux there is reduced by 20%. This indicates that the long-term increase in the freshwater export through the Canadian Archipelago is caused by the freshening of adjacent water masses in the western Arctic Ocean. In contrast, the freshwater import through the Bering Strait is decreased by about 25%. This latter feature is consistent with the freshening of the Arctic Ocean which induces a decrease in the mean meridional pressure gradient between the Pacific and the Arctic Oceans, and therefore weakens the Bering Strait throughflow (Coachman and Aagaard 1966).

Finally, as a consequence of the long-term warming and freshening of the high latitudes of the North Atlantic Ocean, the model predicts that the convection almost disappears in the GIN Seas and south of Iceland by the end of the twenty-first century, with a very shallow ventilation depth in March of about 100–200 m (not shown). However, this does not lead to a complete shut-down of the

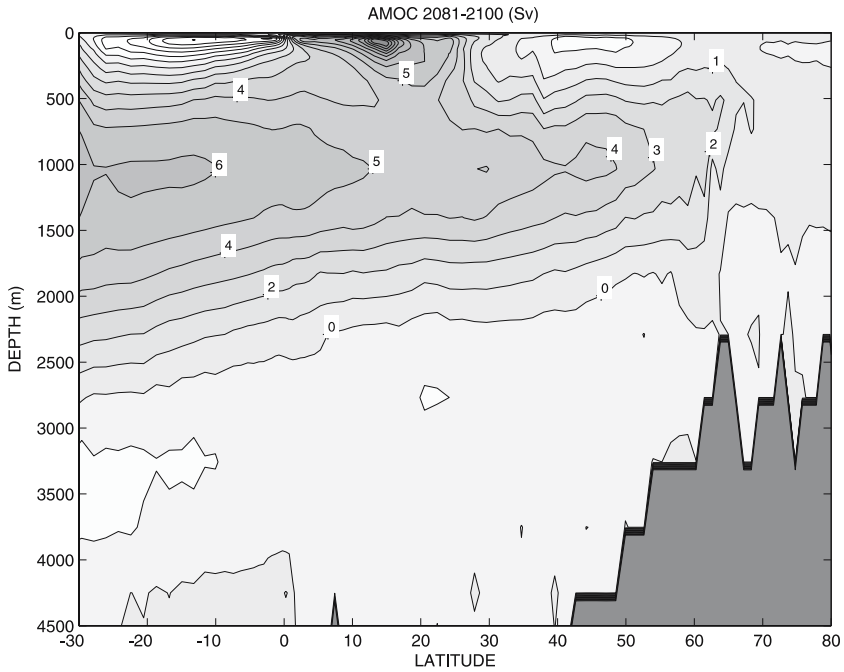

Fig. 5 Annual mean Atlantic meridional overturning circulation (Sv) averaged over 2081–2100. Contour interval is 1 Sv. Shaded positive values indicate anticlockwise circulation

AMOC, as it remains at a value of about 6 Sv by 2100. The structure of the weakened AMOC averaged over 2081–2100 is illustrated in Figure 5. Note finally that the location of deep convection sites over the twenty-first century is the same as the one simulated during the twentieth century (i.e., in the GIN Seas and South of Iceland).

5 Processes influencing the long-term changes in the Fram Strait liquid freshwater flux

About 50% of the total volume of freshwater leaves the Arctic Ocean through Fram Strait (Serreze et al. 2006). This gives a particular importance to this freshwater flux in driving the freshwater storage of the Arctic Ocean, as well as the water mass properties in the GIN Seas and to some extent the overflow into the North Atlantic. In addition, this freshwater outflow may also interact with the Atlantic meridional overturning circulation. Observation-based estimates indicate that about half of the freshwater flux there is liquid (Serreze et al. 2006). Over the late twenty-first century however, our analysis suggests that the liquid freshwater export at Fram Strait might represent a significant contribution (75%) to the total Fram Strait freshwater flux (Fig. 4b). It becomes therefore essential to determine the mechanisms that drive this export, and in particular on time scales at which human influence on climate is most likely to occur. In this section, we specifically focus our analysis on the mechanisms influencing the long-term changes in liquid freshwater export at Fram Strait. Our analysis is based on the experiments covering the twentieth century with anthropogenic forcing and the SRES A1B scenario.

Figure 6 shows the timeseries of the liquid freshwater and volume fluxes at Fram Strait over the twentieth and twenty-first centuries. An interesting feature seen in these timeseries is the rapid strengthening of the volume and freshwater fluxes between 1990 and 2010. Such an abrupt shift is not reproduced in a control simulation with pre-industrial conditions (Fig. 6). This means that the anthropogenic forcing is responsible for this significant change during that period. Furthermore, the volume and freshwater fluxes appear well correlated with a correlation coefficient up to 0.9 over 1901–1980 and 2021–2080 (all fields linearly detrended), suggesting that changes in the Fram Strait volume flux rather than changes in salinity have a significant influence on modifications of the liquid freshwater export at Fram Strait. We therefore investigate hereafter the mechanisms influencing the Fram Strait volume flux rather than those influencing the liquid freshwater export.

5.1 Strengthening of the Fram Strait volume flux

The large shift of the Fram Strait volume flux simulated between 1990 and 2010 (Fig. 6a) can be thought to be initiated by the reduction of sea ice cover in the Barents Sea which appears as a consequence of the long-term warming of the Arctic climate (Fig. 7a). The reduction of the annual mean sea ice cover in the Barents Sea (Fig. 7b) over the late twentieth century amplifies the warming of the overlying atmosphere in this region mainly in winter through the reduced insulating effect of sea ice. This yields

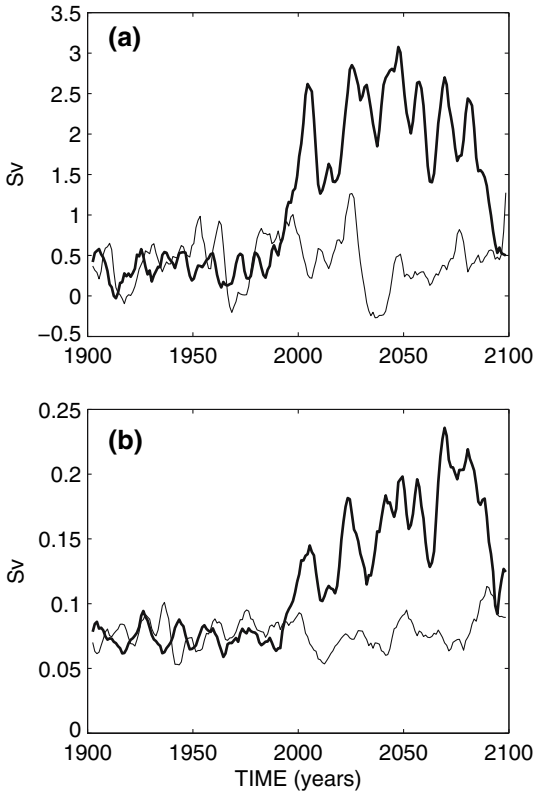

Fig. 6 Timeseries of **a** Fram Strait volume flux and **b** liquid freshwater export at Fram Strait in the pre-industrial experiment (*thin line*) and in the experiment covering the twentieth century with anthropogenic forcings and the SRES A1B scenario over the twenty-first century (*thick line*). A 5-year running mean has been performed to provide clearer timeseries

a decrease of the winter mean (DJF) sea level pressure (SLP) around Spitzbergen (Fig. 7c) causing more cyclonic conditions in the GIN Seas. As a result, the Fram Strait volume flux increases as well as the Barents Sea oceanic heat transport (Fig. 8) which ultimately amplifies the initial sea ice reduction. The increase in the Barents Sea oceanic heat transport reaches 0.02 PW in annual mean between 1901–1980 and 2021–2080 (0.025 PW change in winter) and is similar to those obtained in several models poleward of 70°N in response to a doubling of the CO2 concentration (Holland and Bitz 2003). In our model, the changes in Arctic surface air temperature between 1901–1980 and 2021–2080 are largest over the Barents Sea, with values up to 15°C in winter (Fig 7a) and 9°C in annual mean (not shown). This regional amplification of the warming is consistent with the above positive feedback and the enhanced northward oceanic heat transport into the Barents Sea. Such enhanced sea ice reduction and surface air warming in the Barents-Kara Seas sector was also obtained in the GFDL CM2.0 model in response to a 1% increase in CO_2 concentration (Stouffer et al. 2006). Finally, it should be noted that no similar shifts have been observed over the late twentieth century although the variability of the exchanges between the North Atlantic and the GIN Seas through the Barents Sea has been large during the last decades.

5.2 Weakening of the Fram Strait volume flux

Around year 2080, the model predicts a second transition threshold beyond which the Fram Strait volume flux rapidly weakens (Fig. 6a). There is indeed a competition between the positive feedback described above, that is responsible for the stability of the state in which the Fram Strait volume flux is large, and the impact of the long-term freshening in the GIN Seas. This latter can be measured through the freshwater storage in the GIN Seas which is increased from 8,400 km^3 to 19,300 km^3 between 1951–2000 and 2051–2100. This surface freshening contributes to the stabilization of the water column and thereby decreases the ability of the deep ocean to release heat to the atmosphere. This leads to a regional cooling over the GIN Seas (Fig. 7d). Surface waters subjected to this atmospheric cooling are no longer able to sink and mix with the warmer deep layers during winter. The annual mean sea surface temperature (SST) in the GIN Seas drops by more than 2°C between 2080 and 2100, while the averaged SAT decreases by about 1°C during the same period. The cooling of the surface waters allows a southward expansion of sea ice in the Barents Sea in winter (Fig. 7e). The resulting reduced insulating effect of sea ice during that period contributes to further drop surface air temperatures. The drop in SAT averaged in the Barents Sea reaches 6°C between 2080 and 2100, much larger than over the GIN seas.

Associated with this strong regional cooling is an increase of the winter mean SLP over the GIN Seas (1 hPa change, Fig. 7f) that tends to weaken the cyclonic circulation in the GIN Seas as well as the Fram Strait outflow (Fig. 6) and the Barents Sea oceanic heat transport (Fig. 8). The weakening of the latter further amplifies the initial expansion of sea ice and thus closes the feedback loop. The decrease in the Fram Strait volume flux over 2080–2100 induces a decrease in the freshwater transport out of the Arctic Ocean. As a result, the freshwater storage dramatically increases in the Arctic Ocean during that period, the drop in SSS averaged over the Arctic Ocean being about 2.5 psu by 2100 compared to 2001–2080.

Schaeffer et al. (2004) also obtained a regional cooling south of Spitzbergen between 2060 and 2100 in response to the SRES A1B scenario. The area delineated by the decrease in SAT in their model coincides with the pattern of change in convection depth and expansion of sea ice. In our model however, the pattern of change in SAT is centered over the Barents Sea (Fig. 7d), and coincides clearly

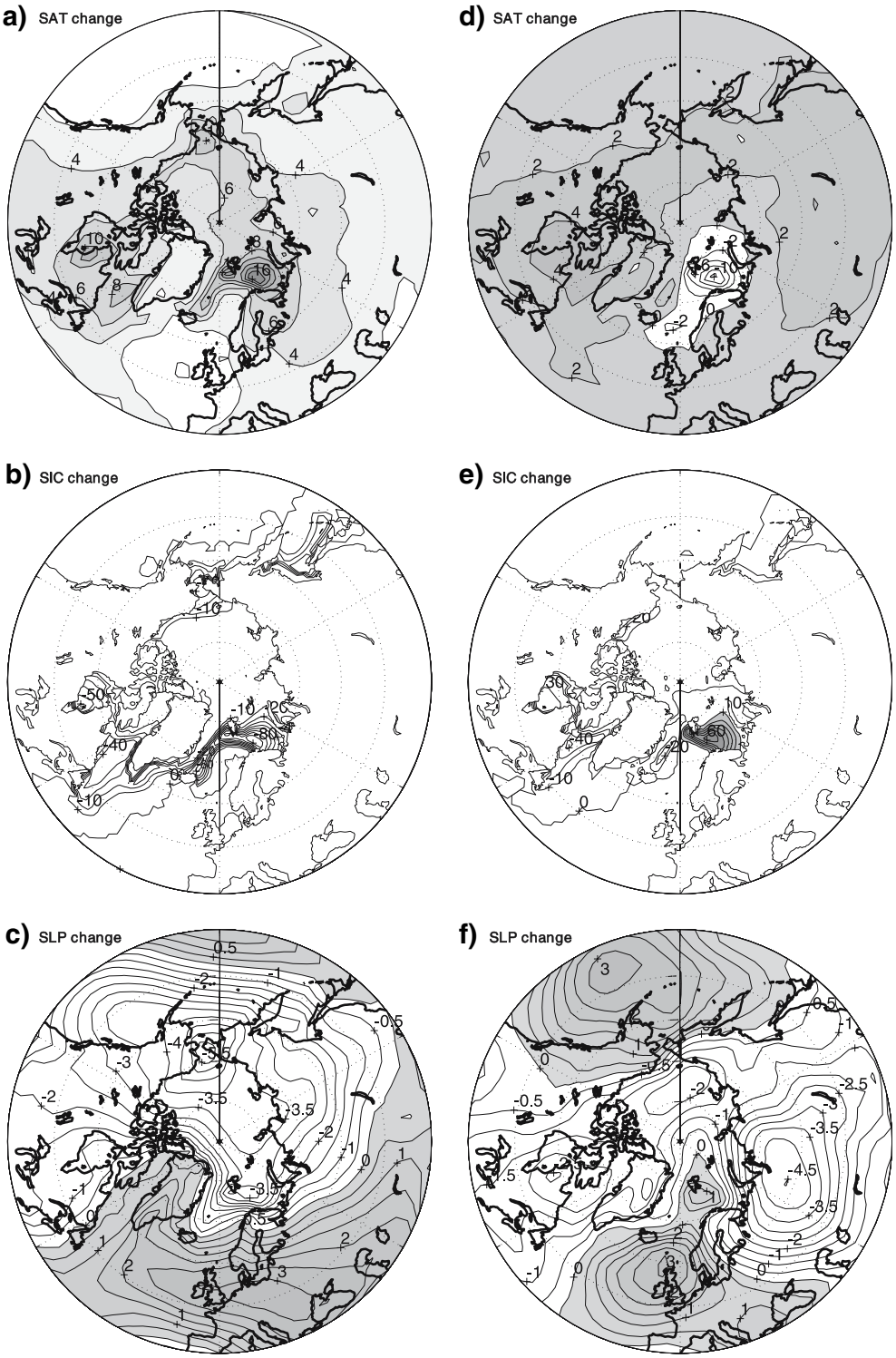

Fig. 7 Change in SAT (c.i 2°C), absolute sea ice concentration (SIC, c.i 0.2), and SLP (c.i 1 hPa) between 2021–2080 and 1901–1980 (**a**–**c**), and between 2091–2100 and 2021–2080 (**d**–**f**). Absolute SIC changes are only calculated in regions where the mean SIC over the initial time period exceeds 15%. Positive values are shaded

with the area of expansion of sea ice (Fig. 7e), the convection changes being located southward in the interior of the GIN Seas. This indicates that the regional cooling in our model is mostly ascribed to the insulating effect of sea ice in winter rather than to a reduced ocean heat loss induced by a collapse of convection.

Those results more or less suggest that there are two stable oscillatory states for the Fram Strait volume (and thus freshwater) flux in the model because of those positive and negative feedbacks. Furthermore, the coarse resolution of our model does not allow to represent all currents, so that we reproduce only strong and weak modes, while in

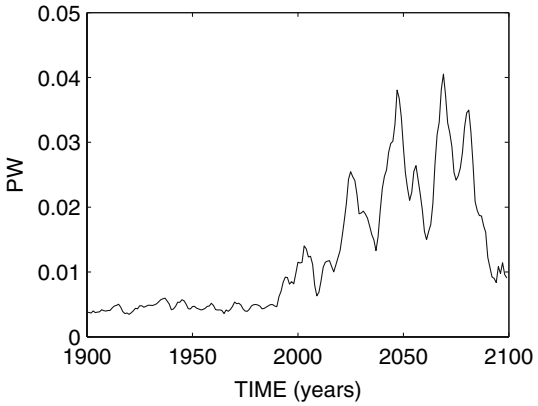

Fig. 8 Timeseries of the simulated oceanic heat transport from the GIN Seas into the Barents Sea. A 5-year running mean has been performed to provide clearer timeseries

reality, the shape of the transition between these stable states could be more continuous. Although those changes do not formally proove causal relationships, they suggest the possibility that the long-term freshening in the GIN Seas could lead to strong regional cooling in a warming climate, through reorganization of horizontal ocean currents and heat transports in agreement with Russell and Rind (1999) and Schaeffer et al. (2002, 2004).

6 Freshwater influence on the interannual variability of deep water renewal

The main objective of this section is to determine whether the processes governing the interannual variability of deep winter oceanic convection in the GIN Seas and South of Iceland over the twentieth century are also valid over the twenty-first century. Special emphasis is placed upon the influence of interannual freshwater fluxes at boundaries enclosing the convection sites. We use detrended timeseries of annual mean freshwater fluxes and March mixed layer depth which is used as a proxy for convection depth. The analysis is performed separately over 1901–1980 and 2021–2080. These peculiar periods have been chosen in order to avoid the periods corresponding to the regime shifts described in Sects. 5.1 and 5.2. The anomalies discussed represent the difference between the simulated field and the linear trend calculated at each grid point over these two periods.

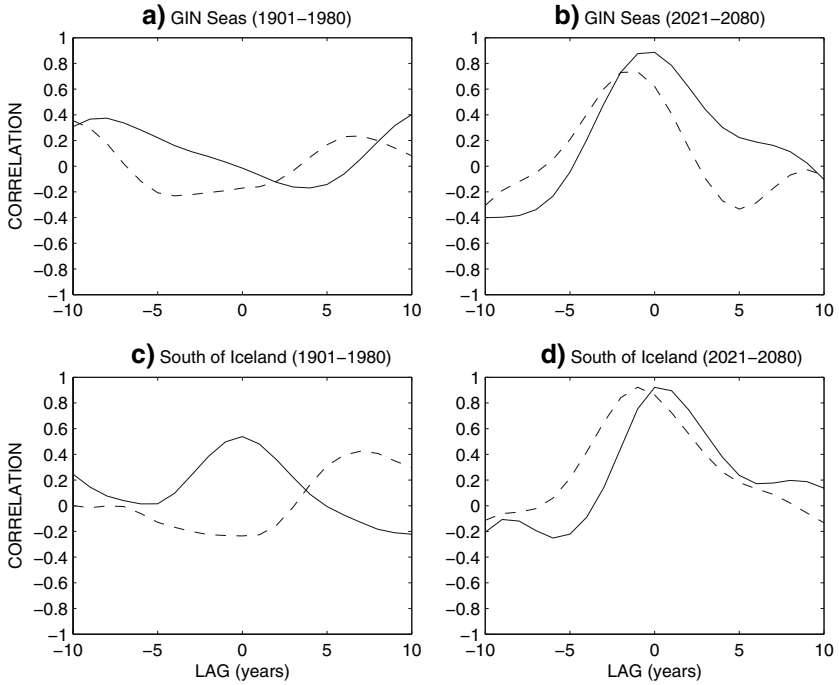

Fig. 9 Correlations between the timeseries of the March mixed layer depth anomalies, defined as the maximum mixed layer depth in the area of interest in March, and the timeseries of the annual mean salinity anomalies averaged in the upper 100 m in the GIN Seas (**a**, **b**) and in the region located south of Iceland (**c**, **d**) as a function of lag over 1901–1980 (**a**, **c**) and 2021–2080 (**b**, **d**). *Solid contours* indicate the correlation between mixed layer depth and upper salinity averaged in the eastern part of the region considered, which correspond to the area where deep convection takes place. *Dashed contours* indicate the correlation between mixed layer depth and upper salinity averaged in the East Greenland Current (**a**, **b**) and in the Irminger Sea (**c**, **d**). Convection anomalies lag (lead) the salinity anomalies for negative (positive) lags. A 5-year running mean has been applied to the detrended timeseries

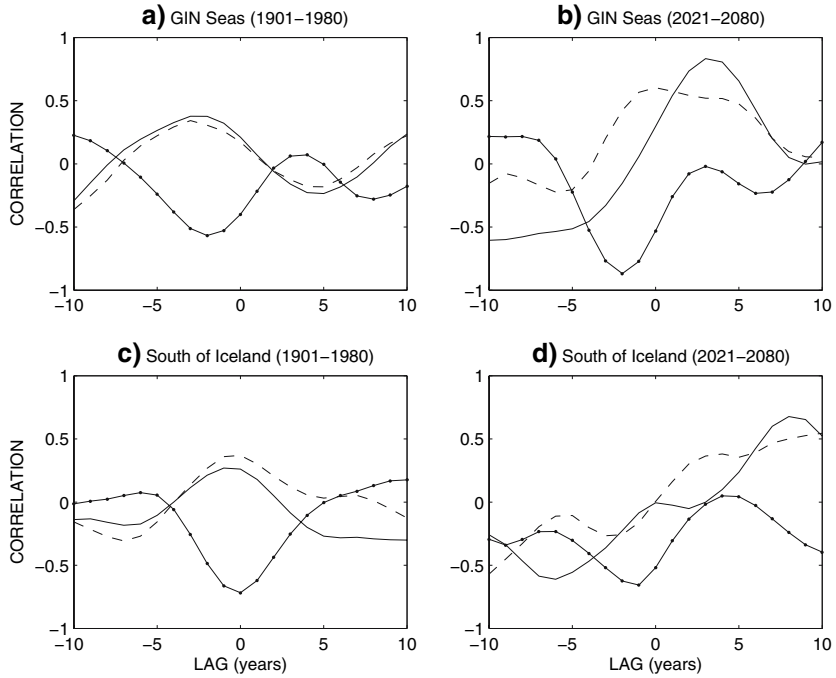

Fig. 10 Correlations between March mixed layer depth anomalies and annual mean oceanic freshwater flux anomalies at boundaries enclosing the GIN seas (**a**, **b**) and the region located south of Iceland (**c**, **d**) as a function of lag over 1901–1980 (**a**, **c**) and 2021–2080 (**b**, **d**). For the GIN Seas, the freshwater fluxes of interest are the liquid and solid ones out of the central Arctic through Fram Strait (*solid* and *dashed*, respectively) and the liquid freshwater import from the North Atlantic through the passage between Iceland and Norway (*solid dotted*). For the region located south of Iceland, the freshwater fluxes considered are the liquid and solid ones through Denmark Strait (*solid* and *dashed*, respectively) and liquid freshwater import from the North Atlantic (*solid dotted*) as a function of lag over 1901–1980 (**c**) and 2021–2080 (**d**). A 5-year running mean has been applied to the detrended timeseries before the analysis. Convection anomalies lag (lead) the freshwater flux anomalies for negative (positive) lags

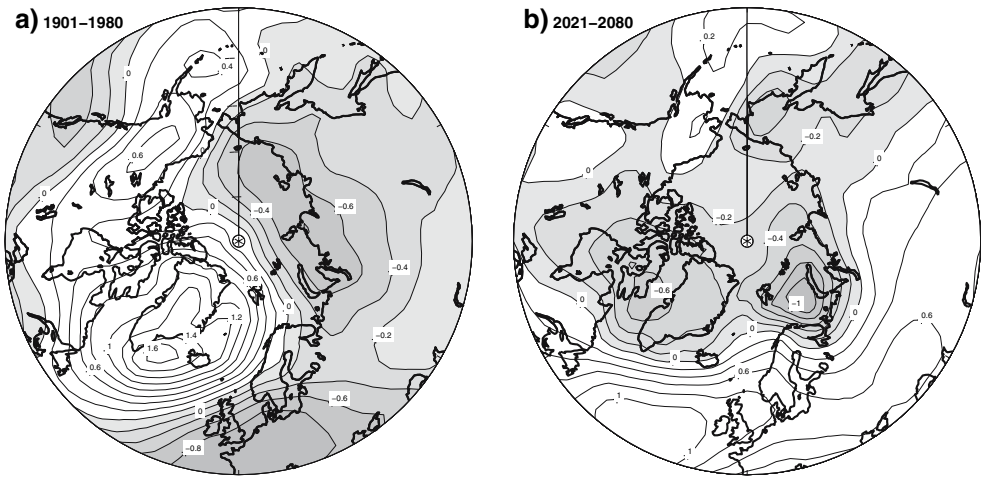

Fig. 11 Winter mean (DJF) SLP anomalies (hPa) regressed upon the timeseries of the annual mean Fram Strait volume flux anomalies over 1901–1980 (**a**) and 2021–2080 (**b**) at zero lag. Shown is the change of SLP related to one standard deviation change in annual mean Fram Strait transport. Contour interval is 0.2 hPa. A linear detrend has been perfomed for SLP and Fram Strait volume flux. Negative values are *shaded*

Statistical significance of lag correlations and regressions analysed in this section are computed by taking into account the autocorrelation of the individual timeseries (Sciremammano 1979). A 5-year running mean has been applied to the timeseries to compute the lag correlations (Figs. 9, 10). Without this time filtering, the correlation values are obviously smaller but remain large enough to provide statistically significant results since the autocorrelation time scales do not exceed 5 years. This allows for a relatively high number of degrees of freedom. A smoothing of the timeseries has instead been chosen purposefully to provide clearer figures. For the computation of the regression maps (Figs. 11, 12, 16, 17) and their associated correlation maps however, no time filtering is applied.

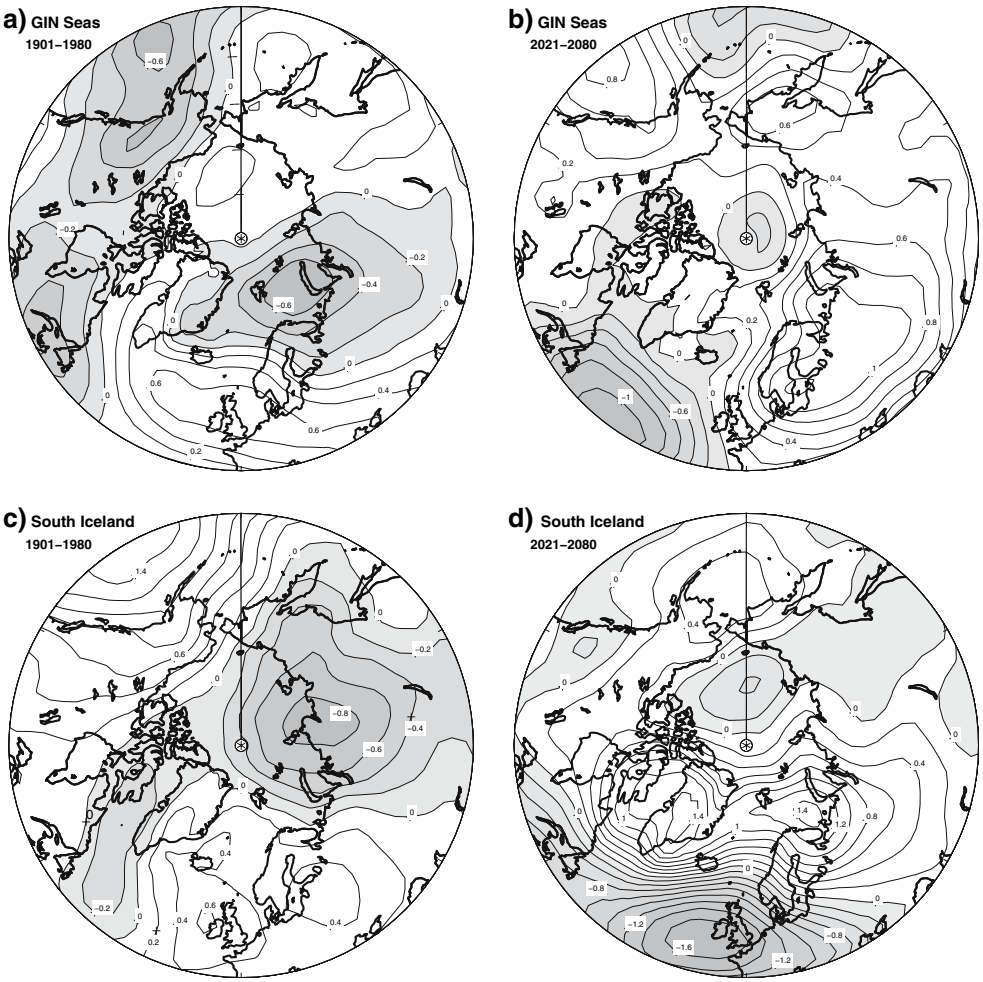

Fig. 12 Winter mean (DJF) SLP (hPa) regressed upon the timeseries of the March mixed layer depth in the GIN Seas and in the region South of Iceland over 1901–1980 and 2021–2080. Shown is the change of SLP related to one standard deviation change in March mixed layer depth. Contour interval is 0.2 hPa. A linear detrend has been performed for SLP and mixed layer depth. Negative values are shaded

6.1 GIN Seas

6.1.1 twentieth century

Figure 9a shows that the correlations between the March mixed layer depth anomalies in the GIN Seas and annual mean salinity anomalies (averaged in the upper 100 m and over the East Greenland Current, EGC) are smaller than 0.3 for all lags between –10 and +10 years. This indicates that freshwater anomalies are not the direct cause of convection depth anomalies during that period. Furthermore, the maximum of the mixed layer depth in the GIN Seas tends to occur about 2 years after a minimum freshwater import from the North Atlantic (Fig. 10a). This is perfectly consistent with the idea that water mass formation in the GIN Seas results from the cooling of warm and salty waters originating from the North Atlantic. On the other hand, the convection depth reaches its maximum about 2 years after the maximum of the southward sea ice and liquid freshwater fluxes at Fram Strait, with a correlation of 0.4 (Fig. 10a). Indeed, almost all sea ice passing through Fram Strait melts close to Iceland over the twentieth century. The subsequent freshwater anomalies are further advected to the North Atlantic and therefore weakly influence the deep convection that takes place in the other parts of the GIN Seas. This is consistent with the regression of winter mean (DJF) SLP upon the timeseries of annual mean Fram Strait outflow (Fig. 11a) which is characterized by a maximum over Greenland (significance 95%). This pattern does not promote eastward advection of freshwater anomalies transported at Fram Strait toward the eastern part of the GIN Seas where deep convection takes place. As a consequence, the convection depth anomalies are not directly related to the influence of the freshwater transport at Fram Strait, but rather to the atmospheric circulation anomalies as discussed below. The spatial structure of this SLP pattern is similar to the dipole anomaly identified by Wu et al. (2006) in the NCEP-NCAR reanalysis dataset. One center is over northern Eurasia and the Arctic marginal seas, and the other is over Canada and Greenland. These authors argued that this dipole anomaly is more important than the Arctic

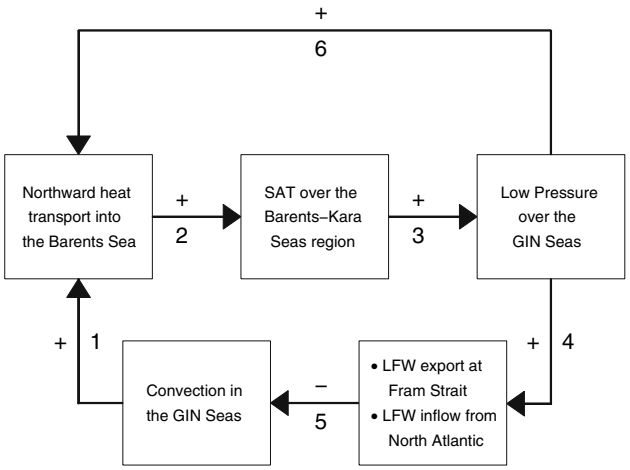

Fig. 13 Sketch of the mechanisms proposed to explain the interannual variability of the convection in the GIN Seas during the twenty-first century. Each interaction between different boxes has been labelled with a number for easier reference in the text. The signs on the arrows are linked with the impact of an anomaly of one variable on the anomaly of the following one. For instance, the sign minus on arrow 5 means that a *positive* freshwater transport out of the central Arctic through Fram Strait induces a *negative* convection depth anomaly in the GIN Seas. LFW states for liquid freshwater. For more details see text

Oscillation for transport of freshwater and ice out of the Arctic Ocean. This is in direct agreement with our results.

The anomalous winter mean atmospheric circulation related to one standard deviation change in convection depth features stronger than usual north-easterly winds in the northern part, and westerly winds in the southern part of the GIN Seas (Fig. 12a). This brings cold air from the Greenland ice sheet and the West Siberian shelf and induces large heat loss in the ice-free regions of the GIN Seas, therefore promoting deep convection there. Furthermore, this atmospheric pattern tends to increase the southward sea ice export through the Fram Strait and explains the positive correlation between sea ice export and mixed layer depth at small negative lags (Fig. 10a).

In addition, when convection is strong, the GIN Seas are characterized by an anomalous cyclonic circulation in agreement with the wind forcing and the large-scale geostrophic adjustment to density increase associated with convection (not shown). This ocean circulation anomaly tends to increase both the inflow of salty Atlantic waters in the GIN Seas and the southward liquid freshwater flux at Fram Strait. The sea ice export at Fram Strait also increases since it is essentially controlled by local wind forcing

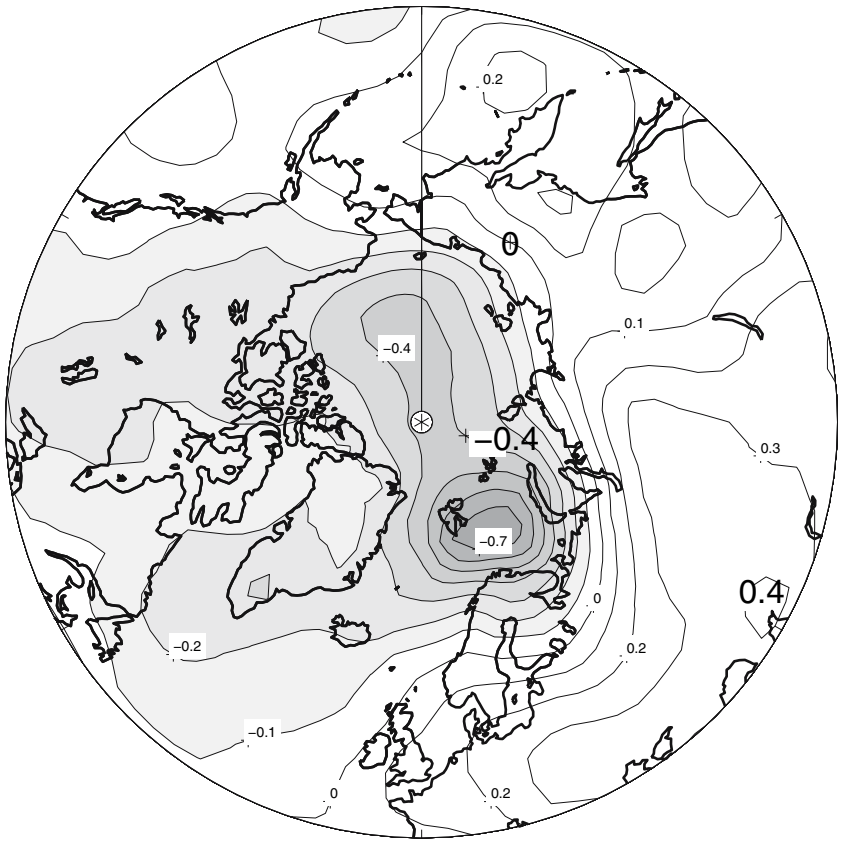

Fig. 14 Winter mean (DJF) SLP regressed upon the timeseries of the winter mean SAT averaged over the Barents Sea area over 2021–2080 at zero lag. Shown is the change of SLP related to one standard deviation change in the Barents Sea SAT (1.35°C over the period). A linear detrend has been performed for SLP and Barents Sea SAT. Negative SLP values are *shaded*

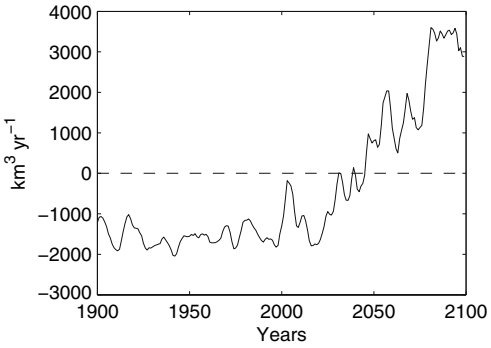

Fig. 15 Timeseries of the North Atlantic freshwater inflow into the GIN Seas, between Norway and Iceland. Negative (positive) values indicate a salty (freshwater) inflow. A 5-year running mean has been applied

(Arfeuille et al. 2000; Vinje 2001; Koenigk et al. 2005). This explains the almost out-of-phase relationship between correlations depicted in Fig. 10a. The results described here strongly support the idea that interannual variability of deep water renewal in the GIN Seas during the twentieth century is driven by the anomalous atmospheric cooling of anomalously salty surface waters.

The coarse resolution of the model could have an influence on the representation of the processes described above as it does not allow accurate representation of the lateral interactions between the East Greenland Current (EGC) and the remaining interior of the GIN Seas. Nevertheless, it should be mentioned that our results are consistent with those from other coarse resolution coupled atmosphere-ocean models (e.g., Goosse et al. 2002). They are also consistent with the conclusions of Mauritzen and Hakkinen (1997), who showed, using a coupled ice-ocean model having a higher resolution that the present one, that the sea ice export at Fram Strait does not significantly influence convection in the GIN Seas.

6.1.2 Twenty-first century

In contrast to the twentieth century, the convection depth anomalies in the GIN Seas during the twenty-first century are strongly positively correlated (0.88, significant at the 99% level) at lag –1 year (convection lags) with the upper salinity anomalies averaged over the EGC (Fig. 9b), and at zero lag with the upper salinity anomalies averaged in the eastern part of the GIN Seas. This indicates that, for this period, salinity anomalies transported in the EGC could induce changes in deep water mass formation or amplify changes caused by other mechanisms. This is confirmed by the correlation between the convection in the GIN Seas and the lateral exchanges of liquid freshwater between the EGC and the interior of the GIN Seas (not shown). The convection is maximum 1 year after the minimum freshwater import from the EGC (correlation –0.6, significance 95%). Furthermore, an increase of deep water formation in the GIN Seas tends to occur a few years after a decrease of the

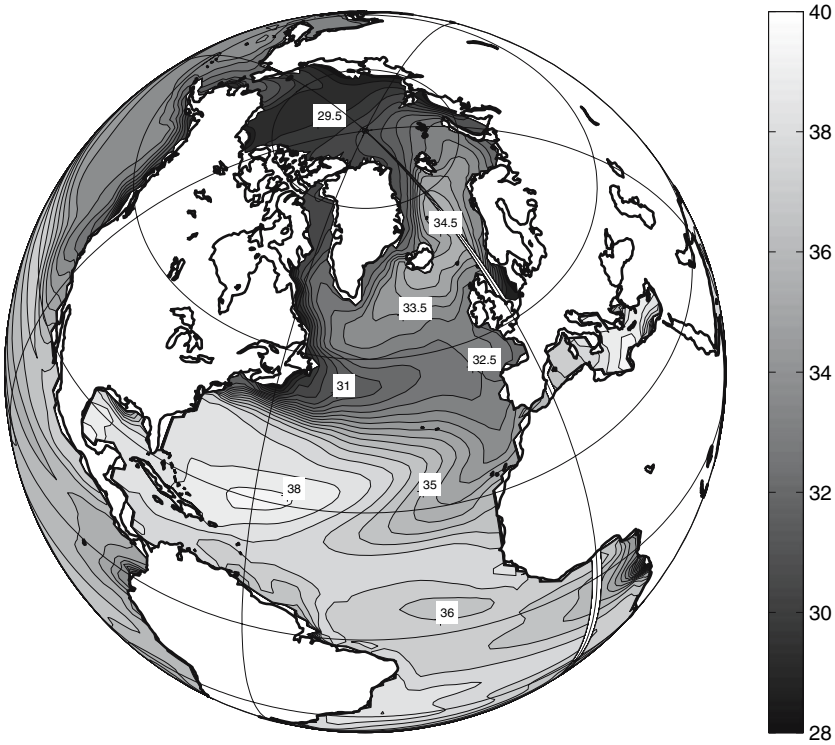

Fig. 16 Annual mean SSS averaged over 2021–2080 (psu). A low salinity tongue is clearly visible at mid-latitudes of the North Atlantic Ocean. Note that the Nordic Seas becomes more saltier than the North Atlantic around year 2045

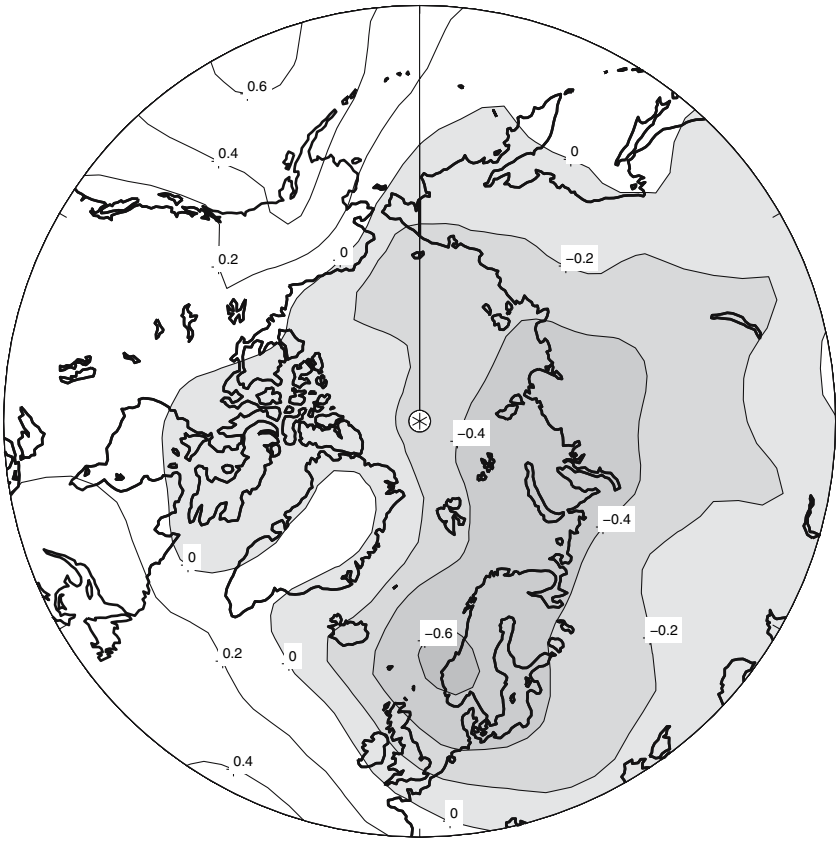

Fig. 17 Annual mean SLP (hPa) regressed upon the timeseries of the March mixed layer depth South of Iceland over 1901–1980. Shown is the change of SLP related to one standard deviation change in March mixed layer depth. Contour interval is 0.2 hPa. A linear detrend has been performed for SLP and mixed layer depth. Negative values are shaded

solid and liquid freshwater export at Fram Strait during the twenty-first century, suggesting that the freshwater anomalies transported at Fram Strait propagate over a few years in the EGC before being exported in the interior of the GIN Seas. This idea is supported by the fact that the winter mean atmospheric circulation associated with a stronger than usual Fram Strait volume flux (Fig. 11b) displays westerly winds in the northern part of the EGC. The correlation reaches 0.35 south of Spitzpergen (significance 90%). This wind forcing promotes lateral exchanges of properties between the EGC and the interior of the GIN Seas over the twenty-first century. Note that no statistically significant correlations are found at small negative lags (convection lags) between the convection and the sea ice import from the EGC into the interior of the GIN Seas (not shown).

In addition, convection leads the freshwater export at Fram Strait by about 4 years with a strong correlation of 0.8 (Fig. 10b), and the freshwater import from the EGC into the interior of the GIN Seas by 6 years with a correlation of 0.7 (both correlations significant at the 95% confidence level). The modifications of the freshwater export at Fram Strait during the twenty-first century might thus potentially be influenced by changes in convection in the GIN Seas. This contrasts with the twentieth century during which a positive convection depth anomaly tends to occur after an increase in freshwater export at Fram Strait. Indeed, the winter mean atmospheric circulation associated with strong convection during the twenty-first century is characterized by southerly winds along the Norwegian coast and in the Barents-Kara Seas sector (Fig. 12b). The correlation reaches 0.4 over the southern part of Norway, significant at the 90% confidence level. This anomalous circulation first brings warm air from the North Atlantic to the Arctic Ocean. Secondly, it leads to larger than usual inflow of warm Atlantic waters in the GIN Seas and in the Barents-Kara Seas area (arrow 1, Fig. 13). In addition to the anomalous northward advection of warm air and warm waters associated with strong convection, the temperature anomalies associated with ocean heat release induced by the convection itself are also transported northward in the Barents-Kara Seas sector by this anomalous atmospheric circulation. All these temperature anomalies then yield a decrease in sea ice cover in the Barents Sea that further warm the overlying atmosphere (arrow 2, Fig. 13). This occurs through the reduced insulating effect of sea ice in winter, the temperature-albedo feedback being very weak during that period of the year. Note that the changes in oceanic heat transport in the Barents Sea does not appear to be influenced by the large-scale AMOC, since the correlation between the AMOC index and the Barents Sea heat transport does not exceed 0.2 for all lags between –10 and

+10 year. This chain of processes is in agreement with the fact that an increase in surface air temperature (SAT) averaged over the Barents Sea occur a few years after an increase in convection depth in the GIN Seas, with a maximum correlation of 0.8 at lag +4. It should be mentioned that it has not been possible to establish a strong relationship between changes in convection and changes in the Barents Sea SAT during the twentieth century. This can be inferred from the atmospheric circulation in Fig. 12a which does not promote an increase in the northward advection of warm air or warm waters in the Barents Sea when the convection is strong.

Let us now examine how the SLP is related to anomalous warm conditions over the Barents Sea during winter. The regression of the winter mean SLP anomalies upon the timeseries of the winter mean SAT anomalies averaged over the Barents Sea is characterized by a clear minimum around Spitzbergen (0.7 hPa), with southward winds at Fram Strait and northeastward winds in the eastern part of the GIN Seas and in the Barents Sea (Fig. 14). The correlation in the Barents Sea is –0.45 (significance 95%). This anomalous atmospheric circulation induces stronger than usual freshwater export through Fram Strait (arrow 4, Fig. 13) that prevents deep convection (arrow 5, Fig. 13), as suggested by the above correlation and regression analyses (Fig. 10b). An auto-correlation analysis of annual mean SSS anomalies indicates that the freshwater anomalies transported at the Fram Strait reach the interior of the GIN Seas with a preferred time scale of about 4 years. An increase in freshwater export at Fram Strait tends to occur therefore after an increase in convection depth in the GIN Seas (Fig. 10b).

Furthermore, this cyclonic circulation anomaly displays southwesterlies between Norway and Iceland. This yields stronger than usual freshwater (instead of salty) import from the North Atlantic that weakens the convection in the GIN Seas, as shown by the correlation depicted in Fig. 10b. Indeed, from year 2045 onwards, the freshwater flux between Norway and Iceland become positive (Fig. 15), indicating that the mid-latitudes of the North Atlantic Ocean feed the Nordic Seas in fresh waters rather than in salty waters from this date on. This feature can also be inferred from the SSS field presented in Fig. 16. A low salinity tongue is clearly visible slightly northward of the southern limb of the sub-polar gyre. It extends from off Newfoundland eastward at mid-latitudes of the North Atlantic Ocean. The increases in the total freshwater transport out of the Arctic Ocean to the North Atlantic through the Canadian Arctic Archipelago (747 km^3 $year^{-1}$, Fig. 4) and the Denmark Strait (1470 km^3 $year^{-1}$) combined with the AMOC weakening and the enhanced hydrological cycle are likely to contribute to the formation of this low salinity tongue of roughly 31 psu during the twenty-first century. The change in SSS averaged in the area of this freshwater tongue between 2021–2080 and 1901–1980 is 1.5 psu. As a result, stronger than usual northward winds between Norway and Iceland during 2021–2080 increase the freshwater inflow rather than the salty inflow in the GIN Seas. This process acts as a negative feedback on the convection in the GIN Seas (similarly to the Fram Strait liquid freshwater flux) when anomalously warm conditions prevail in the Barents Sea region. The convection is minimum 2 years after the maximum freshwater inflow with a significant correlation of –0.8 (Fig. 10b).

The SLP anomaly related to warm conditions in the Barents Sea (Fig. 14) is also associated with southward advection of cold air from the central Arctic that tends to weaken the effect of freshwater on deep convection since salinity effects on deep convection overwhelm those associated with temperature. In addition, this anomalous atmospheric circulation tends to increase the oceanic heat transport in the Barents Sea, as well as the northward advection of warm air from the North Atlantic. This further amplifies the initial SAT anomaly centered over the Barents Sea (arrow 6, Fig. 13) through direct air-sea heat exchanges and intermediate sea ice processes (i.e., insulating effect in winter).

It should be mentioned that we cannot prove from our study if the northward oceanic heat transport into the Barents Sea and the subsequent warming of the the atmosphere are able to influence the SLP around Spitzbergen. Further sensitivity experiments are needed to assess the robustness of our results. However, the winter mean SLP pattern associated to one deviation standard change in Barents Sea SAT (Fig. 14) bears some resemblance with those obtained by Alexander et al. (2004) and Magnusdottir et al. (2004) who analyzed the response of the atmospheric circulation to realistic perturbations of SST and sea ice extent using stand-alone atmospheric general circulation models.

To summarize, the interannual variability of convection in the GIN Seas over the twenty-first century results from the interplay of two major feedbacks: a positive one between the Barents Sea SAT and the Barents Sea oceanic and atmospheric heat transports (arrows 2, 3 and 6, Fig. 13), and a negative one between convection and the freshwater inflow through Fram Strait and from the North Atlantic (arrows 1–5, Fig. 13). The former one was also recognized for the first time by Renssen et al. (2002) in the model of intermediate complexity ECIBilt-CLIO. These authors showed that this positive feedback plays an essential role in the response of the system to a freshwater pulse in the North Atlantic Ocean, and could explain abrupt cooling events such as the one that occured 8.2 kyr ago over Greenland. Using the same model, Goosse et al.

(2003) found that this mechanism lead to the formation of large sea ice volume anomalies. Bengtsson et al. (2004) suggested that such a positive feedback could explain the Arctic warming observed in the mid twentieth century. Finally, Goosse and Holland (2005) identified this positive feedback in the second version of the Community Climate System Model (CCSM2) under present-day conditions with no changes in anthropogenic forcing.

6.2 Region located south of Iceland

6.2.1 twentieth century

Figure 9c shows that the convection depth anomalies south of Iceland are negatively correlated with the upper salinity anomalies averaged in the Irminger Sea (the western part of the box located south of Iceland shown in Fig. 1) with a correlation of –0.2 at zero lag. These correlations are not significant, suggesting that the freshwater content of the Irminger Sea does not influence the convection South of Iceland. This idea is supported by the correlations between changes in annual mean freshwater exports through the Denmark Strait and interannual convection depth anomalies (Fig. 10c). The convection depth reaches a maximum about 1 year after the maximum sea ice and liquid freshwater exports at Denmark Strait indicating that both solid and liquid freshwater fluxes are not the direct cause of the convection anomalies south of Iceland. This contrasts with the studies of Mauritzen and Hakkinen (1997), Hakkinen (1999) and Holland et al. (2001) who argued that convection in the North Atlantic is very sensitive to ice export through the Denmark Strait and its subsequent melting. The convection site in those modelling studies however is located close to the southern tip of Greenland, a region which is directly affected by sea ice export through the Denmark Strait. In contrast, the deep-convection site located south of Iceland in our model is too far eastward of the EGC to be directly influenced by sea ice export through the Denmark Strait.

Close to this narrow passage, the annual mean atmospheric circulation associated with strong convection displays northerlies (significance 95%), as it can be deduced from SLP anomalies shown in Fig. 17. This is consistent with larger than usual southward sea ice and freshwater transports there. In addition, this atmospheric pattern brings cold air from the central Arctic, which further enhances surface ocean heat loss to the atmosphere and thus promotes deep convection south of Iceland. Note that it was not possible to establish a coherent link between the behaviour of the freshwater fluxes at Denmark Strait when the convection is strong (Fig. 10c) and the regression of the winter mean SLP anomalies upon the timeseries of the annual mean convection depth anomalies (Fig. 12c).

In addition, the convection tends to be deep when the upper oceanic layers south of Iceland and east of the Irminger Sea are anomalously salty, with a correlation of 0.5 at zero lag (significant at the 90% confidence level, Fig. 9c). This is consistent with the correlation between the convection depth anomalies and the changes in freshwater import from the North Atlantic, which is strongly negative at zero lag (–0.8, Fig. 10c). Furthermore, the correlation between the convection anomalies and the northward volume flux from the North Atlantic into the convection area peaks at 0.8 at zero lag. These features are in agreement with the regression of the winter mean SLP anomalies upon the timeseries of the annual mean convection depth anomalies (Fig. 12c). The associated wind forcing induces a northward advection of salty waters originating from the North Atlantic. Finally, the changes in upper salinity in this region are mainly related to changes in the upper ocean circulation rather than to variations in the large-scale AMOC. Indeed, the maximum upper salinity averaged in the top 100 m tends to occur 2 years after a minimum of the AMOC index with a correlation of -0.3 that is not statistically significant.

In summary, years characterized by strong convection South of Iceland during the twentieth century are associated with unusual advection of cold air from the central Arctic. This process could act as a preconditionning for deep convection. During winter, when the convection anomalies are largest, stronger than usual southerlies induce enhanced advection of salty waters from the mid-latitudes of the North Atlantic Ocean and promote thereby deep water formation.

6.2.2 Twenty-first century

Similarly to the GIN Seas, years characterized by strong convection south of Iceland during the twenty-first century tend to be associated with anomalously salty conditions (Fig. 9d). The correlations are however much higher than during the twentieth century, suggesting that salinity changes could drive the convection depth anomalies during that period. Figure 10d illustrates the correlations between the maximum mixed layer depth and the freshwater exchanges at the Denmark Strait and with the North Atlantic. Similarly to the twentieth century, the convection is weak 2 years after the maximum freshwater import from the North Atlantic (correlation –0.6, significance 95%). This is perfectly consistent with the combination of the two following features: the winter mean atmospheric circulation associated with strong convection (Fig. 12d) which is characterized by north-easterly winds around the convection area, and the low salinity tongue in the mid-latitudes of the North Atlantic Ocean (Fig. 16). Thus, these features support the idea that positive (negative) convection depth

anomalies south of Iceland during the twenty-first century result from the weaker (stronger) than usual northward advection of *fresh* waters originating from the northwestern part of the North Atlantic. This differs from the variability over the twentieth century. In this case, positive convection anomalies are associated with stronger than usual northward advection of *salty* waters originating from the mid-latitudes of the North Atlantic Ocean.

7 Conclusions

Outputs from IPSL-CM4 have been used to investigate the processes influencing the long-term changes in the freshwater balance of the Arctic Ocean and the mechanisms governing the interannual variability of deep winter oceanic convection over the twentieth and twenty-first centuries. The analyses have been performed on the basis of simulations performed for the IPCC AR4, namely the experiment covering the twentieth century, which includes only anthropogenic forcings, and the SRES A1B scenario over the twenty-first century.

The model predicts that the increases in continental runoff and liquid freshwater import from the North Atlantic through the Barents Sea constitute the major sources of freshening for the Arctic Ocean over the twenty-first century, while freshwater exports through the Fram Strait and the Canadian Arctic Archipelago represent the major sinks. In an effort to increase our understanding of the mechanisms influencing the freshwater release from the Arctic Ocean to the North Atlantic Ocean in a warming climate, we have further analysed the long-term evolution of Fram Strait liquid freshwater flux over the twentieth and twenty-first centuries. Two significant transitions in this freshwater export are found. The first one occurs between 1990 and 2010. We suggest that it is caused by a regional positive feedback in the atmosphere-sea ice-ocean system initiated by the retreat of the sea ice cover in the Barents Sea over the late twentieth century. Over the late twenty-first century, the model predicts a second transition threshold beyond which the Fram Strait volume and freshwater fluxes rapidly weaken. The long-term freshening of the GIN Seas, which indirectly affects the magnitude of the overall above-mentioned positive feedback (through reorganization of deep convection and ocean currents in the GIN seas) is pointed out as the main contender to explain this large shift. The magnitudes of the long-term changes in the Fram Strait volume flux simulated by the model are roughly 2 Sv. These are comparable to the monthly mean fluctuations reported by Fahrbach et al. (2001) using current meter moorings between 1997 and 1999 in Fram Strait. The timing of the first transition (between 1990 and 2010), depends on the timing of the retreat of the winter mean sea ice cover in the Barents Sea resulting from the warming of the Arctic climate. The timing of the second transition (between 2080 and 2100) is intimately related to the establishement of a strong halocline in the GIN Seas, which is itself influenced by vertical oceanic mixing processes, changes in sea ice, local greenhouse warming and modifications of atmospheric and oceanic transports.

The mechanisms governing the interannual variability of deep convection in the Nordic Seas have then been examined over the twentieth and twenty-first centuries on the basis of correlation and regression analyses of detrended variables. This does not allow us to demonstrate causal effects or to assess the relative contributions of various processes in a particular phenomenon. Additional sensitivity experiments will thus be needed to disentangle the feedbacks discussed in this paper. This could be addressed by specifying SST/sea ice anomalies in the Barents Sea with respect to the base state of the twentieth and twenty-first centuries and to compare the responses to the SLP patterns presented in Figs. 12 and 14. However, we were able to show that the mechanisms of interannual variability of deep convection in the GIN Seas and South of Iceland differ fundamentally between the twentieth and twenty-first centuries. The difference is caused by the dominant influence of freshwater over the twenty-first century.

More specifically, the interannual variability of deep convection in the GIN Seas over the twentieth century is driven by the anomalous atmospheric cooling of anomalously warm and salty waters originating from the North Atlantic which is in agreement with observations. Over the twenty-first century however, modifications in the southward freshwater export through Fram Strait, combined with changes in the northward inflow of fresh waters from the North Atlantic, are seen to play a major role (Fig. 13). Conversely, changes in deep convection in the GIN Seas affect the Fram Strait freshwater export through alterations of SLP around Spitzbergen during the twenty-first century. South of Iceland (i.e., the second convection site in the model), years characterized by strong convection during the twentieth century are associated with unusual salty conditions. Stronger than usual southerlies in this region during winter induce enhanced advection of salty waters from mid-latitudes of the North Atlantic Ocean, thereby promoting deep water formation. In contrast, years characterized by strong convection South of Iceland during the twenty-first century are associated with weaker than usual northward advection of fresh waters originating from a low salinity tongue in the northwestern part of the North Atlantic Ocean.

Although the large-scale atmospheric variability, such as the North Atlantic Oscillation (NAO), may influence the exchanges between the Arctic and the Atlantic

Oceans, it does not seem to have a significant impact on the long-term or interannual variability of climate variables simulated in the GIN-Barents Seas region. Instead, the mechanisms are related to regional processes involving interactions in the atmosphere-sea ice-ocean system. For instance, the correlations between changes in convection in the GIN Seas, Fram Strait volume flux or Barents Sea and SLP are not statistically significant in the mid-latitudes of the North Atlantic Ocean, therefore dismissing a potential influence of the NAO. In addition, no statistically significant correlations betweeen these variables and the large-scale AMOC could be found. In contrast, the proximity of the region located south of Iceland with the mid-latitudes of the North Atlantic Ocean makes the interannual changes in convection in this region much more influenced by the NAO.

It should be stressed that our analysis is based on the results of one experiment performed with a particular model. This has the risk that our results are model dependent. The robustness of the mechanisms proposed here need therefore to be reexamined using other climate models. A major drawback of our model is the absence of convection in the Labrador Sea. This model deficiency could have an impact on the reliability of the Arctic climate change simulated by the model during the late twenty-first century. For example, Schaeffer et al. (2004) showed that the location of present-day convection sites in the ocean is crucial for the probability and strength of a regional cooling signal under global warming. The internal variability could also have a strong influence on the timing of abrupt regional cooling in the GIN Seas (Schaeffer et al. 2002), which is responsible for the weakening of the Fram Strait outflow between 2080 and 2100 in our model. Ensemble experiments are therefore needed to assess the probability of such events over the late twenty-first century in our model. In addition, our model does not include a comprehensive Greenland ice sheet model that has yet been shown to have a significant influence on the climate of the late twenty-first century (Fichefet et al. 2003). Because of all these above-mentioned limitations and biases, our results need to be reexamined using other models simulating a realistic present-day climatology.

Nevertheless, several aspects of our results are not is disagreement with previous published results obtained with different coupled models suggesting that similar mechanisms operate. This study suggests that the oceanic freshwater fluxes could drive the changes of North Atlantic deep water formation at interannual time scales during the twenty-first century, and that rapid and strong transitions in the freshwater export out of the Arctic Ocean through Fram Strait could be triggered by a moderate reduction of the sea ice cover in the Barents Sea or by a development of a strong halocine in the GIN Seas, an issue that must be kept in mind when analysing model results and observations in that region.

Acknowledgments Didier Swingedouw kindly provided several Ferret routines for the analysis. We would like to thank Penny Ajani for having made wording suggestions on a final draft of this paper. H. Goosse is Research Associate with the Belgian National Fund for Scientific Research. This work was conducted within the European project ENSEMBLES (ENSEMBLE-based Predictions of Climate Changes and their Impacts) and the Action Concertée Incitative Changement Climatique et Cryosphère funded by the French Ministry of Research.

References

Aagaard K, Carmack EC (1989) The role of sea ice and other fresh water in the Arctic circulation. J Geophys Res 94:14485–14498

Alexander MA, Bhatt US, Walsh JE, Timlin MS, Miller JS, Scott JD (2004) The atmospheric response to realistic Arctic sea ice anomalies in an AGCM during winter. J Clim 17:890–905

Arfeuille G, Mysak LA, Tremblay L-B (2000) Simulation of the interannual variability of the wind-driven Arctic sea-ice cover 1958–1988. Clim Dyn 16:107–121

Bengtsson L, Semenov VA, Johanessen OA (2004) The early twientieth-century warming in the Arctic. A possible mechanism. J Clim 17:4045–4057

Bitz CM, Roe GH (2004) A mechanism for the high rate of sea ice thinning in the Arctic Ocean. J Clim 17:3623–3631

Blindheim J (1989) Cascading of Barents Sea bottom water into the Norwegian Sea. Rapp P-V Reun Const Int Explor Mer 17:161–189

Bryden HL, Longworth HR, Cunningham SA (2005) Slowing of the Atlantic meridional overturning circulation at 25N. Nature 438:655–657

Cavalieri DJ, Parkinson CL, Vinnikov KY (2003) 30-year satellite record reveals contrasting Arctic and Antarctic decadal sea ice variability. Geophys Res Lett 30. doi:10.1029/2003GL018931

Coachman LK, Aagaard K (1966) On the water exchange through Bering Strait. Limnol Oceanogr 11:44–59

Curry R, Dickson B, Yashayaev I (2003) A change in the freshwater balance of the Atlantic Ocean over the past four decades. Nature 426:826–829

Curry R, Mauritzen C (2005) Dilution of the northern North Atlantic in recent decades. Science 308:1772–1774

Dickson B, Yashayaev I, Meincke J, Turrell B, Dye S, Holfort J (2002) Rapid freshening of the deep North Atlantic Ocean over the past four decades. Nature 416:832–837

Dickson KW, Brown R (1994) The production of North Atlantic deep water—sources, rates and pathways. J Geophys Res 12:319–341

Dickson RR, Meincke J, Malmberg S, Lee AJ (1988) The ''Great Salinity Anomaly'' in the northern North Atlantic. Prog Oceanogr 20:103–151

Dickson R, Lazier J, Meincke J, Rhines P, Swift J (1996) Long-term coordinated changes in the convective activity of the North Atlantic. Prog Oceanogr 38:241–295

Dickson RR, Dye S, Karcher M, Meincke J, Rudels B, Yashayaev I (2006) Current estimates of freshwater flux through Arctic and subarctic seas. Prog Oceanogr (in press)

Dufresne J-L, Quaas J, Boucher O, Denvil S, Fairhead L (2005) Contrasts in the effects on climate of anthropogenic sulfate aerosols between the 20th and the 21st century. Geophys Res Lett 32. doi:10.1029/2005GL023619

Emery WJ, Fowler CW, Maslanik JA (1997) Satellite-derived maps of Arctic and Antarctic sea ice motion: 1988 to 1994. Geophys Res Lett 24:897–900

Fahrbach E, Meincke J, Osterhus S, Rohardt G, Schauer U, Tverberg V, Verduin J (2001) Direct measurements of volume transports through Fram Strait. Polar Res 20:217–224

Fichefet T, Morales Maqueda MA (1997) Sensitivity of a global sea ice model to the treatment of ice thermodynamics and dynamics. J Geophys Res 102:12609–12646

Fichefet T, Poncin C, Goosse H, Huybrechts P, Janssens I, Le Treut H (2003) Implications of changes in freshwater flux from the Greenland ice sheet for the climate of the 21st century. Geophys Res Lett 30. doi:10.1029/2003GL017826

Ganachaud A, Wunsch C (2000) Improved estimates of global ocean circulation, heat transport and mixing from hydrographic data. Nature 407:453–457

Goosse H, Holland M (2005) Mechanisms of decadal Arctic climate variability in the Community Climate System Model CCSM2. J Clim 18:3552–3570

Goosse H, Selten FM, Haarsma RJ, Opsteegh JD (2002) A mechanism of decadal variability of the sea-ice volume in the Northern Hemisphere. Clim Dyn 19:61–83

Goosse H, Selten FM, Haarsma RJ, Opsteegh JD (2003) Large sea-ice volume anomalies simulated in a coupled climate model. Clim Dyn 20:523–536

Gregory JM, Dixon KW, Stouffer RJ, Weaver AJ, Driesschaert E, Eby M, Fichefet T, Hasumi H, Hu A, Jungclaus JH, Kamenkovich IV, Levermann A, Montoya M, Murakami S, Nawrath S, Oka A, Sokolov AP, Thorpe RB (2005) A model of intercomparison of changes in the Atlantic thermohaline circulation in response to increasing atmospheric CO_2 concentration. Geophys Res Lett 32. doi:10.1029/2005GL023209

Hakkinen S (1999) A Simulation of thermohaline effects of a great salinity anomaly. J Clim 12:1781–1795

Hansen B, Turrell WR, Osterhus S (2001) Decreasing overflow from the Nordic seas into the Atlantic Ocean through the Faroe Bank channel since 1950. Nature 411:927–930

Holland MM, Bitz CM (2003) Polar amplification of climate change in coupled models. Clim Dyn 21:221–232

Holland MM, Bitz CM, Eby M, Weaver A (2001) The role of ice-ocean interactions in the variability of the North-Atlantic thermohaline circulation

Houghton JT et al (2001) IPCC 2001, Climate Change (2001) The scientific basis, Contribution of Working Group 1 to the third assessment report of Intergovernmental Panel on Climate Change. Cambridge University Press, Cambridge, 881 pp

Hourdin F, Musat I, Bony S, Braconnot P, Codron F, Dufresne J-L, Fairhead L, Filiberti M-A, Friedlingstein P, Grandpeix J-Y, Krinner G, LeVan P, Li ZX, Lott F (2006) The LMDZ4 general circulation model: climate performance and sensitivity to parameterized physics with emphasis on tropical convection. Clim Dyn 19:3445–3482

Jungclaus JH, Haak H, Mikolajewicz U, Latif M (2005) Arctic-North Atlantic interactions and multidecadal variability of the meridional overturning circulation. J Clim 18:4016–4034

Kerr RA (2005) The Atlantic Conveyor may have slowed, but don't panic yet. Science 310:1403–1404

Knight JR, Allan RJ, Folland CK, Vellinga M, Mann ME (2005) A signature of persistent natural thermohaline circulation cycles in observed climate. Geophys Res Lett 32. doi:10.1029/2005GL024233

Koenigk T, Mikolajewicz U, Haak H, Jungclaus J (2005) Variability of Fram Strait sea ice export: causes, impacts and feedbacks in a coupled climate model

Krinner G, Niovy N, Noblet-Ducoudré N, Ogée J, Polcher J, Friedlingstein P, Ciais P, Sitch S, Prentice IC (2005) A dynamic global vegetation model for studies of the coupled atmosphere-biosphere system. Glob Biogeochem Cycles 19, GB1015. doi:10.1029/2003GB002199

Kwok R, Cunningham GF, Pang SS (2004) Fram Strait sea ice outflow. J Geophys Res 109. doi:10.1029/2003JC001785

Latif M, Boning C, Willebrand J, Biastoch A, Dengg J, Keenlyside N, Schweckendiek U (2006) Is the thermohaline circulation changing? J Clim 19:4631–4637

Levitus S, Burgett R, Boyer TP (1994) World Ocean Atlas 1994. Volume 3: Salinity. NOAA Atlas NESDIS 3. US Deptartment of Commerce, Washington, DC

Madec G, Delecluse P, Imbard M, Lévy M (1998) OPA 8.1, Ocean General Circulation Model reference manual, Notes du pôle de modélisation, Institut Pierre-Simon Laplace (IPSL), France, vol 11, 91 pp

Magnusdottir G, Deser C, Saravanan R (2004) The effects of North Atlantic SST and Sea ice anomalies on the winter circulation in CCM3. Part I Main features and storm track characteristics of the response. J Clim 17:857–876

Manabe S, Stouffer RJ (1995) Simulation of abrupt climate change induced by fresh-water input into the North Atlantic Ocean. Nature 378:165–167

Marti O, Braconnot P, Bellier J, Benshila R, Bony S, Brockmann P, Cadule P, Caubel A, Denvil S, Dufresne J-L, Fairhead L, Filiberti MA, Foujols M-A, Fichefet T, Friedlingstein P, Goosse H, Grandpeix J-Y, Hourdin F, Krinner G, Lévy C, Madec G, Musat I, de Noblet N, Polcher J, Talandier C (2005) The new IPSL climate system model: IPSL-CM4. Note du pôle de modélisation, 26, ISSN 1288–1619, 2005. http://www.ig-cmg.ipsl.jussieu.fr/Doc/IPSLCM4/

Mauritzen C, Hakkinen S (1997) Influence of sea ice on the thermohaline circulation in the Arctic-North Atlantic Ocean. Geophys Res Lett 24:3257–3260

Meredith MP, Heywood K, Dennis P, Goldson L, White R, Fahrbach E, Schauer U, Osterhus S (2001) Freshwater fluxes through the western Fram Strait. Geophys Res Lett 28:1615–1618

Moritz RE, Bitz CM, Steig EJ (2002) Dynamics of recent climate change in the Arctic. Science 297:1497–1502

Overland JE, Spillane MC, Soreide NN (2004) Integrated analysis of physical and biological pan-Arctic change. Clim Change 63:291–322

Peterson BJ, Holmes RM, McClelland JW, Vorosmarty CJ, Lammers RB, Shiklomanov AI, Shiklomanov IA, Rahmstorf S (2002) Increasing river discharge to the Arctic Ocean. Science 298:2171–2173

Pickart RS, Straneo F, Moore GWK (2003) Is Labrador Sea Water formed in the Irminger basin? Deep Sea Res 50:23–52

Prinsenberg SJ, Hamilton J (2005) Monitoring the volume, freshwater and heat fluxes passing through Lancaster Sound in the Canadian Arctic Archipelago. Atmos Oceans 43:1–22

Rayner NA, Parker DE, Horton EB, Folland CK, Alexander LV, Rowell DP, Kent EC, Kaplan A (2003) Global analyses of sea surface temperature, sea ice, and night marine air temperature since the late nineteenth century. J Geophys Res 108. doi:10.1029/2000JC000542

Renssen H, Goosse H, Fichefet T (2002) Modeling the effect of freshwater pulses on the early Holocene climate: the influence of the high-frequency climate variability. Paleocanography 17. doi:10.1029/2001PA000649

Rothrock DA, Yu Y, Maykut GA (1999) Thinning of the Arctic sea ice cover. Geophys Res Lett 26:3469–3472

Russel GL, Rind D (1999) Response to CO_2 transient increase in the GISS coupled model: regional coolings in a warming climate. J Clim 12:531–539

Schaeffer M, Selten FM, Opsteegh (2002) Intrinsic limits to predictability of abrupt regional climate change in IPCC SRES scenarios. Geophys Res Lett 29. doi:10.1029/2002GL015254

Schaeffer M, Selten FM, Opsteegh JD, Goosse H (2004) The influence of ocean convection patterns on high-latitude climate projections. J Clim 17:4316–5329

Sciremammano F (1979) A suggestion for the presentation of correlations and their significance levels. J Phys Oceanogr 9:1273–1276

Serreze MC, Coauthors (2000) Observational evidence of recent change in the northern high-latitude environment. Clim Change 46:157–207

Serreze MC, Barrett AP, Slater AG, Woodgate RA, Aagaard K, Lammers RB, Steele M, Moritz R, Meredith M, Lee CM (2006) The large-scale freshwater cycle of the Arctic. J Geophys Res 111. doi:10.1029/2005JC003424

Stouffer RJ, Broccoli AJ, Delworth TL, Dixon KW, Gudgel R, Held I, Hemler R, Knutson T, Lee H-C, Schwarzkopf MD, Soden B, Spelman MJ, Winton M, Zeng F (2006) GFDL's CM2 global coupled climate models. Part IV Idealized climate response. J Clim 19:723–740

Swingedouw D, Braconnot P, Delecluse P, Guilyardi E, Marti O (2006) Sensitivity of the Atlantic thermohaline circulation to global freshwater forcing. Clim Dyn (published online). doi:10.1007/s00382-006-0171-3

Valcke S, Declat D, Redler R, Ritzdorf H, Schoenemeyer T, Vogelsang R (2004) Proceedings of the 6th international meeting: high performance computing for computational science, Universidad Politecnica de Valencia, Valencia, Spain. The PRISM Coupling and I/O System. VECPAR'04

Vellinga M, Wood RA (2002) Global climatic impacts of a collapse of the Atlantic thermohaline circulation. Clim Change 54:251–267

Vinje T (2001) Fram Strait ice fluxes and atmospheric circulation 1950–2000. J Clim 14:3508–3517

Vinje T, Nordlund N, Kvambekk A (1998) Monitoring ice thickness in Fram Strait. J Geophys Res 103:10437–10449

Woodgate RE, Aagaard K (2005) Revising the Bering Strait freshwater flux into the Arctic Ocean. Geophys Res Lett 32. doi:10.1029/2004GL021747

Wu B, Wang J, Walsh JE (2006) Dipole anomaly in the winter Arctic atmosphere and its association with sea ice motion. J Clim 19:210–225

Wu P, Wood R, Stott P (2004) Does the recent freshening trend in the North Atlantic indicate a weakening of the thermohaline circulation? Geophys Res Lett 31. doi:10.1029/2003GL018584

Wu P, Wood R, Stott P (2005) Human influence on increasing Arctic river discharges. Geophys Res Lett 32. doi:10.1029/2004GL021570